Experimental and Modeling Studies of Transport Limitations in Lithium-O_2 Battery

By

Farhad Mohazabrad

B.Sc., Yasuj University (Iran), 2007

Submitted to the graduate degree program in Mechanical Engineering and the Graduate Faculty of the University of Kansas in partial fulfillment of the requirements for the degree of Master of Science.

Dr. Xianglin Li _____

Thesis Advisor Chair

Dr. Christopher Depcik _____

Committee Member

Dr. Lin Liu _____

Committee Member

Date Defended: 15 December 2016

The thesis committee for Farhad Mohazabrad certifies that this is the approved version of the following thesis:

Experimental and Modeling Studies of Transport Limitations in Lithium-O_2 Battery

Committee Chair: Xianglin Li

Date Approved: 15 December 2016

Abstract

The Li-O_2 battery is one of the more promising technologies to meet the ever-growing energy demand of the modern world. The theoretical energy density of Li-O_2 battery could be as high as 2.8 kWh/kg due to the high energy density of anode lithium metal and an unlimited supply of oxygen from ambient air as the cathode active material. However, several technical challenges (e.g. unstable electrolytes, limited mass transport, low round-trip efficiency) remain unsolved and have hindered its commercialization. In this study, experimental and modeling methods are used to investigate mass transport properties of Li-O_2 battery using organic electrolytes. Discharge products (mainly Li_2O_2) are not soluble in organic electrolytes and precipitate at the reaction sites in the porous cathode electrode where the oxygen reduction reaction (ORR) happens. This pore blockage and film formation would further decrease the oxygen and lithium ion transport in the cathode electrode.

A brief introduction to the Li-O_2 battery and its challenges are presented in the first chapter of this study. The second chapter of this study experimentally investigated the influence of the open ratio of the cathode electrode to the oxygen. Throughout this study, the electrolyte solution was prepared by dissolving bis(trifluoromethane)sulfonamide lithium salt (LiTFSI) in tetraethylene glycol dimethyl ether (TEGDME) as the organic electrolyte. Although it was expected that increasing the open ratio would improve the cell performance by increasing oxygen transport, the experimental results showed that other factors, such as electrolyte evaporation and cell contact resistance, also play important roles in determining the discharge/charge capacity of the battery. The electrolyte evaporation rate is a function of oxygen flow rate, oxygen pressure, electrolyte vapor pressure, the open ratio of the oxygen electrode, and protective layers used. The maximum discharge capacity was achieved with 25% open ratio (995 mAh/g_{carbon}) and with 3% open ratio (747 mAh/g_{carbon}) at 0.1 and 0.3 mA/cm^2 discharge currents, respectively, among all tested open ratios (0% - 100%). The effects of initial

amounts of electrolyte and impedance analysis of the battery on discharge and charge performance are also studied in this chapter. In the third chapter of this study, a novel model that considers the evaporation of electrolyte and two distinct regions in commercially available electrodes, gas diffusional layer (GDL) and microporous layer (MPL), has been developed. This model can accurately predict discharge capacities at various open ratios observed by our experiments when the change of the amount of the electrolyte by evaporation is considered. Distribution of oxygen, lithium ions, the rate of the ORR, and the volume fraction of discharge product (Li_2O_2) are presented in this section. In the fourth chapter, the effect of the salt concentration in the electrolyte on the performance of battery at various discharge current densities is experimentally investigated. Various concentrations between 0.005 mole (M) and 1 M were selected and viscosity and ionic conductivity of the electrolyte solution were measured at each salt concentration. Results indicated that discharge and charge capacities, as well as the columbic efficiency, decreased with increasing current density from 0.1 to 0.5 mA/cm^2. At lower current density ($\leq$ 0.2 mA/cm^2), the highest capacity was obtained with the 0.75 M electrolyte, while at a higher current density (0.3-0.5 mA/cm^2), the highest capacity was obtained with 1 M electrolyte. Results also showed that specific discharge and charge capacities of batteries at a very low salt concentration ($\leq$ 0.25 M) were extremely low.

Acknowledgements

I would like to take the opportunity to express my gratitude to all who have made substantial contributions toward completion of my thesis.

First of all, I would like to thank my advisor Dr. Xianglin Li for giving me the opportunity to be a part of this project. In the past two and half years, his patience, expertise, guidance, constructive comments and encouragements have helped me to gain a deeper understanding of the subject and present a higher quality of work.

I also want to thank my thesis committee members, Dr. Lin Liu and Dr. Christopher Depcik for their invaluable insights.

I would like to express my gratitude to my lab mates, especially to Fangzhou Wang, for all the collaborations and helpful discussions.

Finally, I want to thank my parents for their patience, endless moral support and understanding throughout my graduate study.

Table of Contents

List of Tables

List of Figures

Chapter 1. Introduction

The idea of the Li-O_2 battery was first proposed in the 1970s as a possible power source for electric vehicles [1]. Despite the potential of this technology, it did not draw much attention from market and scientists at that time due to risks and issues embedded with the technology. In 1996, Abraham and Jiang [2] proposed an improved and rechargeable Li-O_2 battery using nonaqueous electrolyte as the solvent. This battery consisted of a thin Li metal foil, a thin solid electrolyte membrane, and a thin carbon composite electrode with high surface area. This promising improvement recaptured researchers' interest in the late 2000s due to ever-growing energy demand, fast depletion of fossil fuels increasing prices of fossil fuels and the global climate change associated with a large amount of carbon dioxide (CO_2) and greenhouse gas released to the atmosphere from these fuels.

There are numerous applications that can benefit from a greater energy storage system: e.g. electric vehicles, power grid storage, and portable electronic devices. The current state of the art Li-ion battery, has greatly improved after its first commercial release by Sony in 1991. The energy density of a Li-ion battery can reach up to 400 Wh/kg [1]. However, this is insufficient to drive an all-electric vehicle for 300 miles with a reasonable battery weight. On the other hand, a nonaqueous Li-O_2 battery has a theoretical specific energy of 12 kWh/kg, excluding oxygen mass. This energy density is about 2.8 kWh/kg when the mass of both electrodes and electrolyte are taken into account [3]. This high specific energy results from the high energy density of the Li anode and the fact that the positive electrode active material, oxygen, is readily available from the surrounding air.

Most of Li-O_2 batteries consist of three main parts: Li anode, a separator (saturated with the electrolyte), and a porous oxygen cathode. In discharge cycle, as shown in Fig. 1-1, the lithium metal is oxidized, electrons transfer in the external circuit to provide electric power,

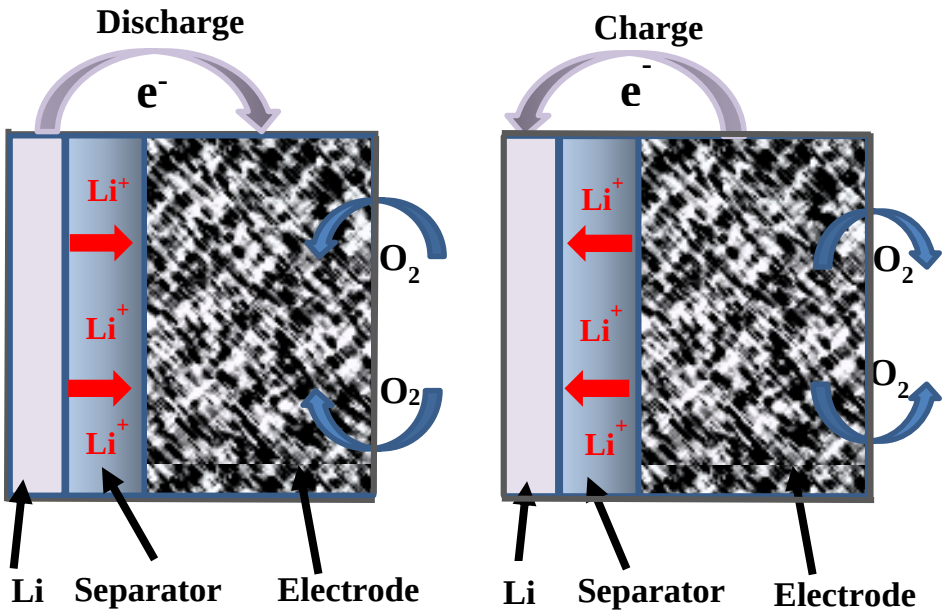

Fig. 1-1. Schematic of the Li-O_2 battery charge and discharge cycle

and lithium ions migrate through the electrolyte to react with the reduced oxygen on the surface of the oxygen electrode. Discharge products, mainly lithium peroxide (Li_2O_2), are non-solube in organic electrolytes and deposit in cathode electrode pores where the electrochemical reaction occurs. During a charging process, external electrical power is applied to decompose discharge products and release oxygen and lithium ions, during which lithium metal deposits on anode electrode. The anode and cathode discharge half reactions are presented in Eqs. 1-2 and Eq. 3 shows the overall discharge reaction with a theoretical voltage, E^0, of 3.1 V when organic electrolyte is used:

$$\text{Anode: } 2Li \rightarrow 2Li^+ + 2e^- \quad (1)$$

$$\text{Cathode: } 2Li^+ + 2e^- + O_2 \rightarrow 2Li_2O_2 \quad (2)$$

$$\text{Overall: } 2Li + O_2 \rightarrow 2Li_2O_2 \quad (3)$$

The charge reaction is simply the reverse of Eq. 1-3. However, even in the absence of any side reactions, several other chemical and electrochemical reactions can be realized as the result of the paired Li-O_2. These reactions are presented in Fig. 1-2 and details of these reactions are found in the original work by Lu et al. [1]. In the most experimental studies, dry oxygen is used

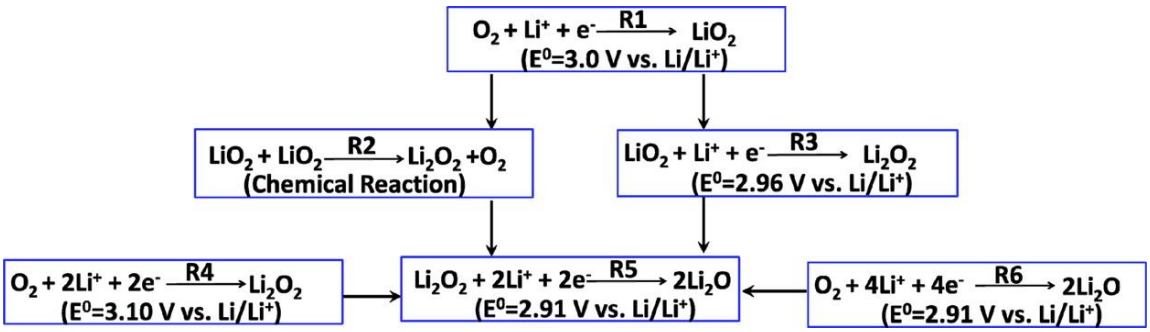

Fig. 1-2. Possible chemical and electrochemical reactions for Li-O_2 couple with no side reactions. Reprinted from [1].

as the cathode active material to minimize the side reactions. However, in the ambient operated Li-air batteries where oxygen is absorbed from the surrounding air, several side reactions may also take place because of the existence of H_2O and CO_2 in the air. These additional side reactions are usually irreversible and deteriorate the battery performance. Additional components, e.g. oxygen selective membrane, are needed when the battery operates in ambient air to limit the electrolyte contamination and evaporation.

Li-O_2 batteries are divided into four categories based on the electrolyte used: the aprotic electrolyte which is also referred to as non-aqueous or organic electrolyte in the literature (non-aqueous electrolyte include both aprotic and protic electrolyte), the aqueous electrolyte, the mixed aprotic and aqueous electrolyte, and the solid state electrolyte [1,4]. Using an organic electrolyte alleviates the anode corrosion caused by water in comparison with aqueous electrolytes. But on the other hand, discharge products (e.g. Li_2O and Li_2O_2) are not soluble in organic electrolytes and deposit in the cathode electrode (mostly in the vicinity of air) where the ORR occurs. Once pores are blocked or a film of solid products is built up in the oxygen electrode, the discharge process stops because of a restricted oxygen transfer to the reaction sites.

The electrolyte is the key factor that determines main electrochemical reactions. An aqueous solvent has the advantage of dissolving the discharge reaction products in H_2O and eliminating the cathode blockage by solid precipitation as it occurs in aprotic electrolytes. Two

basic reactions are reported for the aqueous electrolyte, depending on the selection of the solvent, acidic or alkaline[5]:

$$2Li^+ + \left(\frac{1}{2}\right) O_2 + 2H^+ \rightarrow 2Li^+ + H_2O \quad \text{(acidic media)} \tag{4}$$

$$2Li^+ + \left(\frac{1}{2}\right) O_2 + H_2O \rightarrow 2LiOH \quad \text{(alkaline media)} \tag{5}$$

Discharge products in acidic solution are dependent on the selection of the acid: e.g., LiCl when NH_4Cl is used and Li_2SO_4 when H_2SO_4 is used as part of the acidic solution [1]. However, batteries using an aqueous electrolyte have far less theoretical energy density than those using aprotic electrolytes [3]. Another disadvantage of using an aqueous electrolyte battery is the undesired reaction between lithium metal and water, which requires the development of a protective layer for the lithium metal. For the aforementioned reasons, this study focused on Li-O_2 batteries using an aprotic electrolyte.

The oxygen electrode is a porous material with a high electric conductivity. The porous electrode is typically made from carbon cloth or carbon paper coated with mixtures of carbon materials (e.g. carbon Super P, Ketjen Black, Acetylene Black, etc.) incorporating different binders, such as Polytetrafluoroethylene (PTFE) or Polyvinylidene fluoride (PVDF). The carbon loading of the electrode can be adjusted by applying a different amount of mixture as the coating. The wettability of the electrode can be adjusted by changing the ratio of binder and porous carbon. In some cases, a catalyst such as λ-MnO_2 is also added to the electrode to improve the round trip efficiency (i.e., the energy released versus stored during a discharge-charge cycle). Oxygen electrode properties such as porosity, specific surface area, pore size distribution and materials, play an important role in the battery performance. It was shown that discharge reactions mainly occur in pores within the mesopore range (2-50 nm) [6–8], while larger pores perform as microchannels for oxygen transfer. Xiao et al. [9] reported a hierarchically porous graphene electrode that facilitated oxygen diffusion through microporous channels to the nanoscale pores where the Li-O_2 reaction takes place. Li and Faghri [10] used

a transient two-dimensional model to show that a better specific capacity can be achieved by redesigning the cathode porosity distribution to have a higher porosity at the air side and lower porosity at the anode side. This concept was experimentally examined by Tan et al. [11] and it was shown that implementing a porosity gradient in the electrode increased the discharge capacity by improving oxygen transfer.

Lithium metal has a very high specific capacity and is an ideal candidate for the anode material. A summary of specific discharge capacity and energy of selected battery systems are presented in Table 1-I [12]. Lithium has 3862 mAh/g specific capacity compared with 1489 mAh/g for aluminum and 820 mAh/g for zinc. Despite the high specific capacity of the lithium metal, there are a few technical challenges that need to be addressed in order to develop a safe and rechargeable Li-O_2 battery. The first is the growth of lithium dendrites due to non-uniform lithium deposition-dissolution during repeated discharge-charge cycles [13]. This leads to the loss of lithium and solvent species which compromise the rechargeability of the Li-O_2 battery and also can cause safety issues due to possible short circuits between two opposite electrodes through dendrites. The second issue is the coverage of lithium anode with a solid electrolyte interface (SEI) layer. This layer is mainly consisted of the electrolyte salts [14]. A thin layer of the SEI is lithium ion conductive and discharge-charge cycles can continue. This SEI layer can fracture and reform after multiple discharge-charge cycles due to volume and morphological

Table 1-I. Theoretical specific capacity and energy (excluding molecular mass of the oxygen) of selected battery systems. Reprinted from ref. [12], Copyright 2007 IUPAC

Metal-air and Li-ion systems (organic or aqueous electrolyte solution)	OCV (V)	Specific energy (Wh/kg)	Specific capacity (mAh/g)
$2Li + ½O_2 \rightarrow Li_2O$ (aprotic organic sln)	2.913	11 248[a]	3862
$Li + ½O_2 \rightarrow ½Li_2O_2$ (aprotic organic)	2.959	11 425[a]	3862
$2Li + ½O_2 + H_2SO_4 \Leftrightarrow Li_2SO_4 + H_2O$	4.274	1091[a]	255
$2Li + ½O_2 + 2HCl \Leftrightarrow 2LiCl + H_2O$	4.274	3142[a]	366
$2Li + ½O_2 + H_2O \Leftrightarrow 2LiOH$	3.446	5789[a]	1681
$Al + 0.75O_2 + 1.5H_2O \rightarrow Al(OH)_3$ (aq)	2.701	4021[a]	1489
$Zn + ½O_2 \rightarrow ZnO$ (aq)	1.650	1353[a]	820
$x6C + LiCoO_2 \Leftrightarrow xLiC_6 + Li_{1-x}CoO_2$	~4.2	420[b]	139

change of the anode surface [15]. This can further lead to uneven deposition of the Li ions and also dendrite formation.

Suggested mechanisms of Li anode morphology changes during Li deposition and Li dissolution are presented in Fig. 1-3 [13]. As shown in this figure, the morphology change is affected by the current density. The anode surface film can accommodate the dissolution and deposition of the Li^+ ion at low current densities. But at a high current density, the surface film cannot accommodate this surface volume change. The anode surface breaks during discharge and then it is repaired by surface reactions of Li with electrolyte solution species. During a charge process, Li is deposited unevenly on the anode electrode, which leads to cracked surface film and dendrite formation.

In the last few decades, several research directions have been studied to alleviate the lithium dendrite formation. It was found that electrolyte solvents and salts can greatly influence this qrowth. In general, an electrolyte-salt solution that results in a more elastic SEI layer is more favorable. Aurbach et al. [14] suggested 1,3-dioxolane as the best solvent because of the

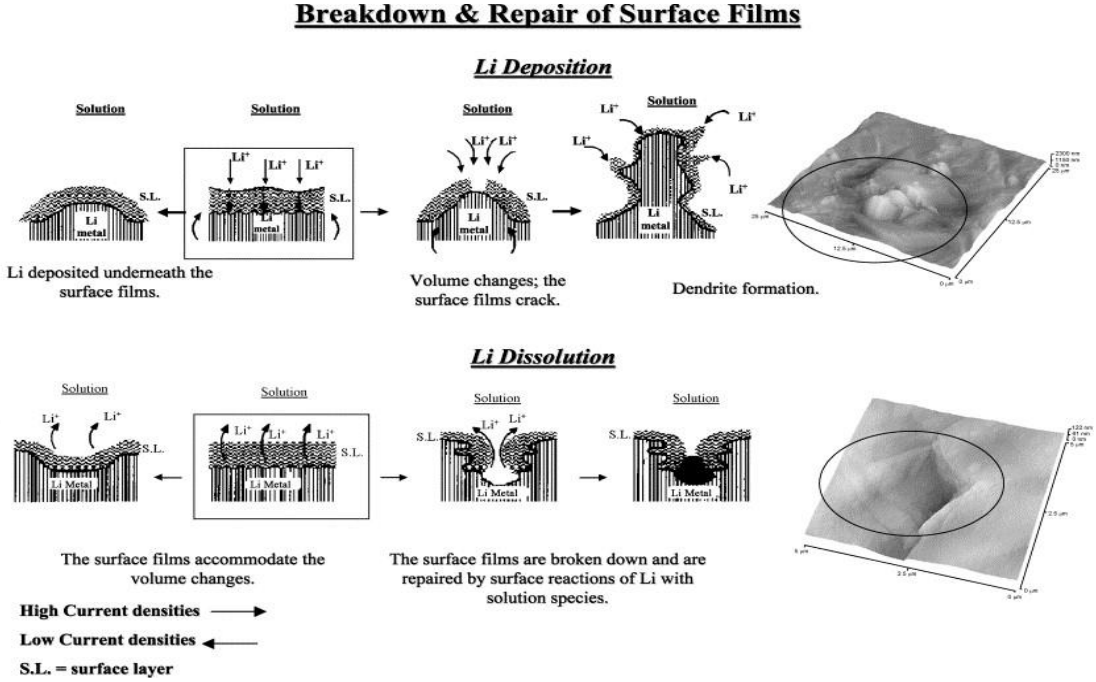

Fig. 1-3. A description of the morphology and failure mechanisms of lithium electrodes during Li deposition and Li dissolution (Li electrodes in an EC-DMC/$LiPF_6$ solution). Reprinted from Ref. [13]. Copyright 2002 ELSEVIER.

formation of oligomers on Li surface. Whereas, ether based electrolytes and ethylene carbonate (EC) solvents are suggested by Wang et al. [16]. Among different lithium salts, $LiPF_6$, LiTFSI, and $LiAsF_6$ are found to improve cycling efficiency and reduce the dendrite formation [17]. Polymer electrolyte, electrolyte additive, lithium alloys (e.g., Li-Al, Li-Na and Li-Mg), working temperature, and battery assembly pressure studies have been accomplished in an effort to reduce the dendrite formation and a summary of the results can be found in a review study by Shao et al. [18].

Besides the technical challenges at the lithium anode, the performance (capacity, current, power etc.) of the Li-O_2 battery is also limited by the mass transfer of oxygen and lithium ion within the porous electrode. Read et al. [19,20] showed that solubility and diffusivity of oxygen in organic electrolytes played a critical role in determining the discharge capacity of Li-O_2 batteries. Because of limited diffusivity of oxygen in the organic electrolytes, the majority of the oxygen reduction reaction (ORR), occurred at the cathode air side and at the oxygen

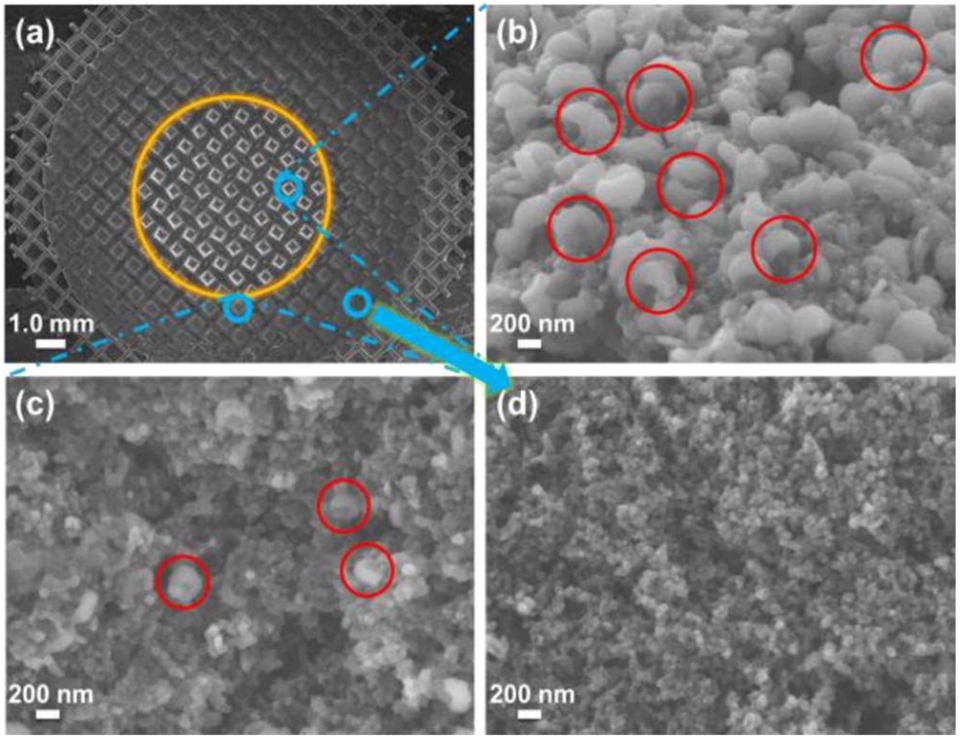

Fig. 1-4. SEM images of discharged electrode: (a) entire morphology, (b) exposure to oxygen, (c) near the edge of the oxygen window, and (d) far away from the oxygen window. Reprinted from [21]. Copyright 2016 ACS.

opening window. Jiang et al. [21] have demonstrated the non-uniform distributions of the reaction product by SEM images in Fig. 1-4 after the battery is discharged to 2.0 V. The oxygen opening window trace is marked with an orange circle in Fig. 1-4a, and Fig. 1-4b shows the areas that were directly exposed to the oxygen, Fig. 1-4c shows the areas near the edge of the oxygen window and Fig. 1-4d shows the area away from the oxygen window. A bulk deposition of the discharge products was clearly clustered inside the oxygen window and the amount of discharge products rapidly decreased at the edge of the oxygen window and diminished further from the oxygen window. This evidence is consistent with findings from previous studies [12,19,22] that Li-O_2 batteries fail due to heavy deposition of Li_2O_2 at the cathode oxygen side and pore blockage. The interior pores of the cathode electrode remain unused due to the reduced oxygen flux from the ambient oxygen after a film of solid product was built at the electrode/oxygen interface after discharge. This shows that mass transfer plays a critical role in determining Li-O_2 battery specific capacity and performance.

Several studies have focused on possible methods to improve the mass transfer of the species in the oxygen electrode to improve the battery performance. For example, the effect of oxygen pressure was studied [23,24], and results indicated that increasing the oxygen pressure promoted the oxygen transfer and improved the discharge capacity from 1390 mAh/g_{carbon} to 2100 mAh/g_{carbon} when the oxygen pressure increased from 1 atm to 10 atm at 0.1 mA/cm^2. Ye et al. [25] developed an analytical model and showed that a thin cathode with large porosity was more favorable to increase the oxygen diffusion, and a wetted cathode can increase the oxygen diffusion and battery performance in comparison with a flooded electrode. Li and Faghri [10] developed a transient two-dimensional model to study the effects of discharge current, cathode porosity distribution, cathode thickness, and cathode open ratio.

In recent years, modeling methods are more commonly used to better understand the mass and charge transfer inside the battery components and their interconnection with

electrochemical reactions. Modeling studies help to examine new ideas and solutions in a timely and economical manner. However, due to the complexity of the mass transfer and electrochemical processes in Li-O_2 batteries, modeling results always need to be examined by experimental methods. The experimental results can be used to optimize the model and add more details to improve the modeling methods to achieve a more precise and reliable simulation result. Details of different macroscopic modeling methods can be found in a recent work of Li et al. [26]. In this study, the macroscopic method was used and details of the equations used in our study will be explained in the following chapters. The rate of ORR is a function of the availability of the reaction sites at the interface between the solid electrode, which transfers electrons, and the liquid electrolyte, which transfers lithium ions and dissolved oxygen. Transport equations are used to determine the concentration of lithium ion and oxygen at each computational domain and each time step. The amount of Li_2O_2 is used to update the porosity, diffusivity, and active surface area of the electrode. All these properties are correlated and their governing equations are solved simultaneously.

Despite all the progress in the last two decades, there are still many challenges remaining before a rechargeable, ambient operated Li-O_2 battery can be developed:

- A stable electrolyte solvent with low boiling point and high oxygen diffusivity can improve the battery capacity significantly.
- Batteries with non-aqueous electrolytes suffer from pore blockage and reduced oxygen diffusivity: therefore, an electrolyte with a higher solubility of discharge products, Li_2O_2, is highly desired.
- A compatible Li salt with high ionic conductivity and low side reactions needs to be developed.
- Improvements of mass transfer properties of oxygen electrodes can provide a better oxygen diffusion pathways and promote better utilization of the electrode.

- A more stable catalyst against oxygen, electrolyte, and intermediate reactants with low cost needs to be developed.
- A more effective protective layer against the air contaminations (mainly H_2O and CO_2) needs to be developed before the battery can safely be used under ambient condition.

The focus of this study is to assess some possible methods to improve the oxygen and lithium ion transfer within the cathode electrode. In the second chapter of this work, the influence of the open ratio of the oxygen electrode current collector is studied experimentally. The subject of this study is to find the optimum open ratio to improve the discharge capacity. Discharge products are deposited at the cathode/oxygen interface and discharge reaction stops due to film formation at this interface. It is expected that one can increase the discharge capacity of the battery by increasing the cathode contact surface area to oxygen by increasing the cathode open ratio. In the third chapter, a numerical model is developed to study the effects of the open ratio, as well as the effect of evaporation as a possible explanation of the experimental results. In the fourth chapter, the effect of Li salt concentration on battery performance at different discharge current densities has been studied experimentally. Lithium ion diffusivity is higher than the oxygen, and it is believed that the oxygen diffusivity is the main limiting factor for battery discharge capacity. Electrolyte viscosity and ionic conductivity are decreased when the lithium salt concentration is decreased in the electrolyte; whereas, diffusivity is increased by decreasing viscosity. The optimized salt concentration is the balance of these two adverse effects. In this chapter, some properties of the electrolyte are measured and optimized salt concentrations for various current densities are determined.

Reference

[1] J. Lu, L. Li, J.-B. Park, Y.-K. Sun, F. Wu, K. Amine, Aprotic and aqueous Li-O2 batteries, Chemical Reviews. 114 (2014) 5611–5640.

[2] K. Abraham, Z. Jiang, A polymer electrolyte-based rechargeable lithium/oxygen battery, Journal of The Electrochemical Society. 143 (1996) 1–5.

[3] J. Zheng, R. Liang, M. Hendrickson, E. Plichta, Theoretical energy density of Li-air batteries, Journal of The Electrochemical Society. 155 (2008) A432–A437. doi:10.1149/1.2901961.

[4] J. Yuan, J.-S. Yu, B. Sundén, Review on mechanisms and continuum models of multi-phase transport phenomena in porous structures of non-aqueous Li-Air batteries, Journal of Power Sources. 278 (2015) 352–369.

[5] G. Girishkumar, B. McCloskey, A. Luntz, S. Swanson, W. Wilcke, Lithium- air battery: promise and challenges, The Journal of Physical Chemistry Letters. 1 (2010) 2193–2203.

[6] X. Yang, P. He, Y. Xia, Preparation of mesocellular carbon foam and its application for lithium/oxygen battery, Electrochemistry Communications. 11 (2009) 1127–1130.

[7] T. Kuboki, T. Okuyama, T. Ohsaki, N. Takami, Lithium-air batteries using hydrophobic room temperature ionic liquid electrolyte, Journal of Power Sources. 146 (2005) 766–769.

[8] J. Xiao, D. Wang, W. Xu, D. Wang, R.E. Williford, J. Liu, et al., Optimization of air electrode for Li/air batteries, Journal of The Electrochemical Society. 157 (2010) A487–A492.

[9] J. Xiao, D. Mei, X. Li, W. Xu, D. Wang, G.L. Graff, et al., Hierarchically porous graphene as a lithium-air battery electrode, Nano Letters. 11 (2011) 5071–5078.

[10] X. Li, A. Faghri, Optimization of the cathode structure of lithium-air batteries based on a two-dimensional, transient, non-isothermal model, Journal of The Electrochemical Society. 159 (2012) A1747–A1754.

[11] P. Tan, W. Shyy, L. An, Z. Wei, T. Zhao, A gradient porous cathode for non-aqueous lithium-air batteries leading to a high capacity, Electrochemistry Communications. 46 (2014) 111–114.

[12] I. Kowalczk, J. Read, M. Salomon, Li-air batteries: A classic example of limitations owing to solubilities, Pure and Applied Chemistry. 79 (2007) 851–860.

[13] D. Aurbach, E. Zinigrad, Y. Cohen, H. Teller, A short review of failure mechanisms of lithium metal and lithiated graphite anodes in liquid electrolyte solutions, Solid State Ionics. 148 (2002) 405–416.

[14] D. Aurbach, Review of selected electrode-solution interactions which determine the performance of Li and Li ion batteries, Journal of Power Sources. 89 (2000) 206–218.

[15] J. Christensen, P. Albertus, R.S. Sanchez-Carrera, T. Lohmann, B. Kozinsky, R. Liedtke, et al., A critical review of Li/air batteries, Journal of the Electrochemical Society. 159 (2011) R1–R30

[16] X. Wang, E. Yasukawa, S. Mori, Electrochemical behavior of lithium imide/cyclic ether electrolytes for 4 V lithium metal rechargeable batteries, Journal of The Electrochemical Society. 146 (1999) 3992–3998.

[17] D. Aurbach, I. Weissman, A. Zaban, O. Chusid, Correlation between surface chemistry, morphology, cycling efficiency and interfacial properties of Li electrodes in solutions containing different Li salts, Electrochimica Acta. 39 (1994) 51–71.

[18] Y. Shao, F. Ding, J. Xiao, J. Zhang, W. Xu, S. Park, et al., Making Li-Air Batteries Rechargeable: Material Challenges, Advanced Functional Materials. (2012). doi:http://dx.doi.org/10.1002/adfm.201200688.

[19] J. Read, Characterization of the lithium/oxygen organic electrolyte battery, Journal of The Electrochemical Society. 149 (2002) A1190–A1195.

[20] J. Read, K. Mutolo, M. Ervin, W. Behl, J. Wolfenstine, A. Driedger, et al., Oxygen transport properties of organic electrolytes and performance of lithium/oxygen battery, Journal of The Electrochemical Society. 150 (2003) A1351–A1356.

[21] J. Jiang, H. Deng, X. Li, S. Tong, P. He, H. Zhou, Research on Effective Oxygen Window Influencing the Capacity of Li-O2 Batteries, ACS Applied Materials \& Interfaces. 8 (2016) 10375–10382.

[22] K. Xu, Nonaqueous liquid electrolytes for lithium-based rechargeable batteries, Chemical Reviews. 104 (2004) 4303–4418.

[23] E.J. Nemanick, R.P. Hickey, The effects of O 2 pressure on Li-O 2 secondary battery discharge capacity and rate capability, Journal of Power Sources. 252 (2014) 248–251.

[24] X. Yang, Y. Xia, The effect of oxygen pressures on the electrochemical profile of lithium/oxygen battery, Journal of Solid State Electrochemistry. 14 (2010) 109–114.

[25] L. Ye, X. Wang, W. Lv, J. Fei, G. Zhu, Y. Liang, et al., Analytical insight into the oxygen diffusion in wetted porous cathodes of Li-air batteries, Energy. 93 (2015) 416–420.

[26] X. Li, J. Huang, A. Faghri, A critical review of macroscopic modeling studies on Li O 2 and Li-air batteries using organic electrolyte: Challenges and opportunities, Journal of Power Sources. 332 (2016) 420–446.

Chapter 2. Influence of Oxygen Electrode Open Ratio and Electrolyte Evaporation on the Performance of Li-O_2 Batteries, Experimental Study

This chapter has experimentally investigated the influence of the cathode electrode open ratio (ratio between oxygen opening area and total electrode surface area) on the performance of Li-O_2 battery at various discharge current densities. Oxygen diffusers with various open surface areas, made from highly corrosion-resistant Grade 2 Titanium, were used at the cathode oxygen side to change the open ratio between 3% and 100%. Specific capacities at the first discharge-charge cycle were measured at current densities of 0.1 and 0.3 mA/cm^2. At the current density of 0.1 mA/cm^2, the maximum discharge capacity was achieved at 25% open ratio among the selected open ratios for this experiment. As the open ratio increased from 25% to 100%, the specific discharge capacity decreased from 995 to 397 mAh/g_{carbon}. The maximum discharge capacity at 0.3 mA/cm^2 was obtained at a much lower open ratio of 3% among tested open ratios. Discharge capacity decreased from 747 to 228 mAh/g_{carbon} when the open ratio increased from 3% to 100%. Open area modulates availability of the oxygen and evaporation of the electrolyte while also impacts contact resistance. The electrolyte was prepared with 1M concentration of bis(trifluoromethane)sulfonamide lithium salt (LiTFSI) dissolved in tetraethylene glycol dimethyl ether (TEGDME). The fast evaporation of the electrolyte can be the main reason for the decrease of the discharge capacity with increasing open ratio at a relatively high open ratio (above 25%). The contact resistance of the battery versus open ratios of the oxygen electrode was also measured by the electrochemical impedance spectroscopy (EIS). The almost linear increase of ohmic resistance from 3.97 Ω to 7.02 Ω when the open ratio increased from 3% to 95% also contributes to the decrease of discharge capacity.

Introduction

Efficient energy storage devices with high energy capacity are demanded more than ever before due to advancements in portable electronic devices and electric vehicles (EV). Fossil fuels are the main source of carbon dioxide (CO_2) and greenhouse gas (GHG) emissions, which cause global climate change and increase the potential for weather disasters (e.g. storms and droughts) all over the world. Transportation is one of the main sources of GHG emissions. Moving to all-electric vehicles will generate 25% less GHG than a conventional gasoline vehicle, considering current U.S. electric generation is a mix of fossil fuels, nuclear, and renewable energy sources [1]. GHG emissions will be further reduced in the future when more renewable energies are used to produce a higher percentage of electricity. Li-ion batteries have been used in numerous applications (e.g., portable electronic devices, power tools, and EVs) after their first introduction by Sony in 1991. Although Li-ion battery technology has significantly improved in the last two decades, its specific capacity is still too low to electrify vehicles and achieve a 300-mile driving range per single charge at a reasonable battery weight [2]. The current state-of-the-art Li-ion battery weighs about 500 kg to achieve a driving range of 300 miles [3,4]. On the other hand, metal-air batteries offer high energy densities, mainly because the cathode active material, oxygen, is not stored in the battery. Among all the tested metal-air batteries, Li-O_2 battery has the highest theoretical energy density of 12 kWh kg^{-1} if oxygen mass is not considered. Li-O_2 batteries have attracted extensive research after Abraham and Jiang [5] developed the first rechargeable Li-air battery using organic electrolytes.

Based on the electrolyte used, Li-O_2 batteries are divided into four categories: the aprotic electrolyte, the aqueous electrolyte, a mixed aprotic and aqueous electrolyte, and the solid state electrolyte [1,4]. The aprotic electrolyte is also referred to as non-aqueous or organic electrolyte in the literature (non-aqueous electrolytes include both aprotic and protic electrolytes). The organic electrolyte alleviates the anode corrosion caused by water compared to batteries using

aqueous electrolytes. However, discharge products (e.g., Li_2O and Li_2O_2) are not soluble in organic electrolytes and all these products deposit in the cathode (mostly on the air side) where the oxygen reduction reaction occurs. The discharge process can cease because of insufficient oxygen transfer to reaction sites caused by pore blockage or film built up in the oxygen electrode.

The chemical and electrochemical reactions involved in aprotic Li-O_2 batteries are complex and are greatly dependent on the salt, electrolyte, discharge and charge current, and cutoff voltages. During the discharge process, lithium metal decomposes to electrons and lithium ions. Lithium ions dissolve in the electrolyte and go through the separator to the cathode electrode. Electrons go through an external circuit to the cathode electrode. Absorbed oxygen at the cathode from ambient air incorporate these electrons and are reduced to negative ions and then react with lithium ions from the anode at the surface of catalysis and carbon electrode. Electric energy is produced by transport of electrons in the external circuit. The two-electron reaction presented in Eq. 1 is the main oxygen reduction reaction (ORR) under normal operating conditions [5], and is the only reaction considered for the purpose of this study.

$$2Li^+ + 2e^- + O_2 \leftrightarrows (Li_2O_2)_S \quad E_{rev} = 2.96\ V \tag{1}$$

There are still many technical challenges to be solved before the mass production of Li-O_2 batteries, including a quantitative understanding of the electrochemical reactions, development of stable electrolytes, improvement of air cathodes and lithium anodes, and air breathing membranes [6]. Read et al. [7,8] showed that solubility and diffusivity of oxygen in organic electrolytes play a critical role in determining discharge capacity of Li-O_2 batteries. It was also shown that discharge capacity can be improved by reformulation of electrolyte or by increasing oxygen pressure to increase the oxygen concentration in electrodes flooded with electrolyte. Development of an electrolyte with a high oxygen solubility and diffusivity is one of the greatest challenges that limits the capacity of Li-O_2 batteries. Ideal electrolytes should meet the

following requirements to be suitable for ambient operation [1,9]: (1) stability against superoxide radical (O_2^-), which is an intermediate phase formed in ORR; (2) high salt solubility, which means a high dielectric constant; (3) low volatility, or high boiling point to reduce the electrolyte loss; (4) low viscosity, which improves ion transport and oxygen diffusivity; (5) stability against all the battery components: Li metal, separator and cathode; and (6) environmental friendly, non-toxic and economical. Many investigations focused on discovering the most compatible electrolyte and salt for Li-O_2 batteries [5,10–15]. There are many other studies on micro and macro structural improvements for the purpose of mass transfer enhancement.

The effect of oxygen pressure was studied [16,17] and results indicated that increasing the oxygen pressure promoted the oxygen transport and improved the discharge capacity from 1390 mAh/g_{carbon} to 2100 mAh/g_{carbon} when the oxygen pressure increased from 1 atm to 10 atm at 0.1 mA/cm^2. It was verified by SEM images that more surface area of the cathode was used, and discharge products were denser at the higher O_2 pressure. The influence of porosity distribution is experimentally examined by Tan et al. [18] and it is showed that implementing a gradient porous cathode with high porosity at the air cathode side and lower porosity at the separator side can increase the discharge capacity by improving oxygen transfer while a high surface area is retained.

Xu et al. [15] studied properties of different electrolytes. Unlike the sealed batteries, Li-O_2 battery is open to the environment and so electrolyte evaporation rate plays a critical role in the battery performance. This study showed that electrolytes with a higher boiling point had a lower evaporation rate. The evaporation rate of dimethyl ether (DME), which has a low boiling point of 85 ^oC, was 87% in just two days while the evaporation rate of propylene carbonate (PC), which has a high boiling point of 240 ^oC, was only 4.8% in 63 days. However, electrolytes

with high boiling point typically have a high viscosity and low ionic conductivity, which result in higher ohmic and mass transfer over-potentials [19].

Recently, Jiang et al. [20] conducted an experimental research on effects of oxygen window on the capacity of Li-O_2 battery. In this work, a single hole with different diameters was machined on the oxygen side of a coin type cell battery to obtain different open ratios of the oxygen electrode. The battery consisted of a homemade electrode, a glass fiber separator, a Li anode and 50 µL of tetraethylene glycol dimethyl ether (TEGDME) as the organic electrolyte solution. All batteries were tested in an oxygen-filled glass chamber at 25 ^{o}C and 1 atm during discharge-charge cycles. In this work, the diameter of the electrode gas diffusional layer was 14 mm (153.9 mm^2), the diameter of the catalytic layer was 12 mm diameter (113.1 mm^2), while the area of the oxygen window varied between 3.14 and 22 mm^2. Therefore, the calculated open ratio (ratio between oxygen window area and total electrode surface area) in this work varied between 2.8% and 19.5%. The first discharge-charge cycle of the Li-O_2 batteries at a current of 0.09 mA/cm^2 showed that battery capacity increased linearly with the size of the oxygen window: from approximately 1 to 6.6 mAh when the size of the oxygen window increased from 3.14 to 22 mm^2.

Similar to Li-ion battery packages, practical Li-O_2 battery packages should be composed of thousands of single batteries to meet the power, current, and voltage requirements of the electronic devices. Therefore, uniform distributions of oxygen among batteries by actively supplying oxygen through flow plates, which is similar to fuel cells, are required. The active supply of oxygen to battery electrodes with open ratios much higher than 20% is foreseeable in future battery applications [21]. Due to the importance of oxygen transfer within the electrode on the electrochemical performance of batteries, this experimental investigation focused on the effect of the open ratio of the oxygen electrode in a wide range (0% to 100%) on Li-O_2 battery performance. Unlike the most previous studies that have stored batteries in a

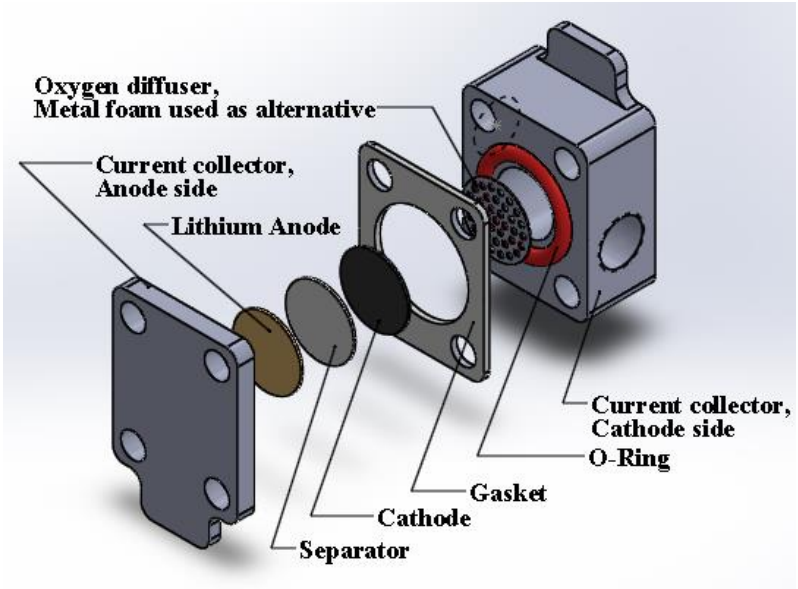

Fig. 2-1. Battery frame and components.

limited space container during a discharge-charge cycle, this experiment constantly supplied oxygen, 0.1 sccm, through the oxygen electrode. The evaporation rate of the electrolyte is a function of oxygen flow rate and the cathode open ratio. In addition, experiments at different discharge current densities have been carried out to further demonstrate the relation between the influence of open ratio, current density, and battery specific capacity. Furthermore, electrochemistry impedance spectroscopy (EIS) has been implemented to explain the influence of the open ratio of the current collector at the oxygen side on the ohmic over-potential and also oxygen diffusion kinetics. We have also developed a two-dimensional computational fluid dynamics model in a separate study to investigate the importance of the electrolyte level change on the performance of the battery at different open ratios [22]. The electrolyte level change in the model was driven by the evaporation and anode volume change. The simulated discharge capacities are in a good agreement with the experimental results. The model serves as a powerful tool to explain the trend observed in this experimental study and to understand multi-phase transport phenomena in porous battery electrodes.

Experiment

Battery grade solvent, TEGDME (99%), and electrolyte salts, Bis(trifluoromethane)sulfonimide lithium salt (LiTFSI, 99.95%), were purchased from Sigma-Aldrich and used as received. All the electrolytes, salts, and other battery materials were stored in a Mikrouna glovebox filled with purified argon. The concentration of the oxygen and water in the glovebox are less than 1 ppm all the time. Electrolytes were prepared by dissolving 1M of LiTFSI in TEGDME in the glovebox.

The oxygen electrode was made from commercially available carbon cloth as the gas diffusional layer (GDL) coated with a microporous layer (MPL) on one side, purchased from the Fuel Cell Store. The total thickness of the electrode is 410 μm of which approximately 110 μm is the MPL coating. A Whatman GF/B glass fiber filter with the diameter of 2.1 cm was used as the separator. The lithium discs with the diameter of 1.56 cm were purchased from MTI Corporation. The frame design of the battery is shown in Fig. 2-1. The battery consisted of two current collectors, anode electrode (Li metal), cathode electrode (oxygen electrode), a gasket (to prevent short between two electrodes), an O-ring (to seal the battery), and also a separator.

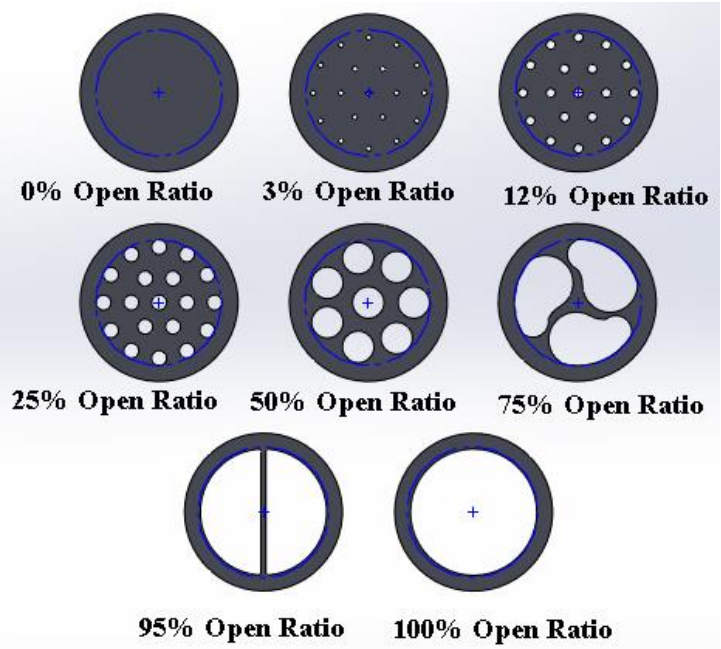

Fig. 2-2. Oxygen diffusers with different open ratios: 0%, 3%, 12%, 25%, 50%, 75%, 95% and 100%.

Two valves were installed at the inlet and outlet of cathode electrode current collector to purge oxygen before discharge, to supply oxygen during discharge-charge cycle tests, and to seal the battery when it was transferred from the glovebox to the test station. The current collectors on both the anode and cathode sides were customer-designed and made from highly corrosion-resistant Grade 2 titanium purchased from McMaster-Carr. The PTFE gasket and O-ring were purchased from McMaster-Carr as well. All batteries were assembled in the glove box by adding totally 150 μL of electrolyte on the separator and the oxygen electrode before they were sandwiched between two current collectors. In order to test the open ratio of the oxygen electrode, an oxygen diffuser disc made from highly corrosion-resistant Grade 2 titanium sheet, purchased from McMaster-Carr, was placed between the current collector and the oxygen electrode. The oxygen diffuser is manufactured with 0%, 3%, 12%, 25%, 50%, 75%, 95% and 100% open ratio, by increasing the number and diameter of the holes in the titanium disc as shown in Fig. 2-2. The dashed circle indicates the size and location of electrode placement.

Assembled batteries were moved to the test station with all the valves (stainless steel ball-valve from McMaster-Carr) closed to prevent air and moisture contamination. After all

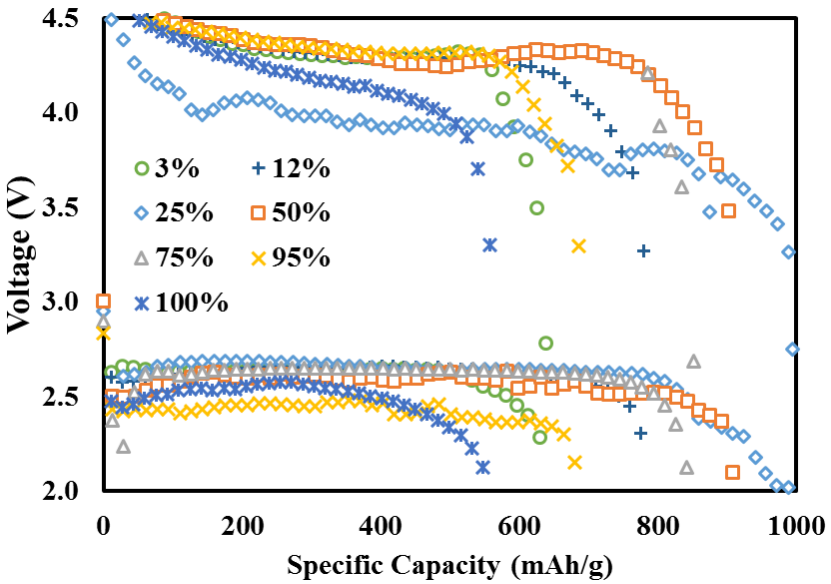

Fig. 2-3. The first discharge charge cycles of Li-O_2 batteries at 0.1 mA/cm^2 current density with 1 M electrolyte at different oxygen diffuser (current collector) open ratios.

batteries are connected to a pure oxygen supply with less than 1 ppm of water content (Matheson Tri-Gas), all batteries were purged by pure oxygen at 2 sccm for 30 s and rested for two hours before starting the discharge and charge cycles. During a discharge and charge process, the pressure of the pure oxygen is maintained at 10 kPa gauge pressure using a pressure controller (T-68027-64, Cole-Parmer) and a flow controller (T-32907-55, Cole-Parmer). The average flow rate of oxygen during the test was 0.1 sccm. The discharge-charge tests were conducted using a 4-channel Arbin MSTAT4 battery tester at room temperature. The cut-off potentials were 2 V and 4.5 V for discharging and charging, respectively. All the batteries are discharged and charged at a constant specific current of 0.1 mA/cm^2 or 0.3 mA/cm^2. All the EIS tests were carried out with SP-150 Potentiostat from BioLogic Science Instrument. The EIS data was analyzed with EC-Lab software (V11.02). All impedance measurements are performed using 10 mV input signal relative to the open circuit voltage of the battery from 100 mHz to 1 MHz.

Experimental Results

The polarization of Li-O_2 batteries with 1 M salt concentration of LiTFSI in TEGDME as the electrolyte under the oxygen pressure of 10 KPa, at current density of 0.1 mA/cm^2 are presented in Fig. 2-3. It should be noted that each test had been repeated at least three times

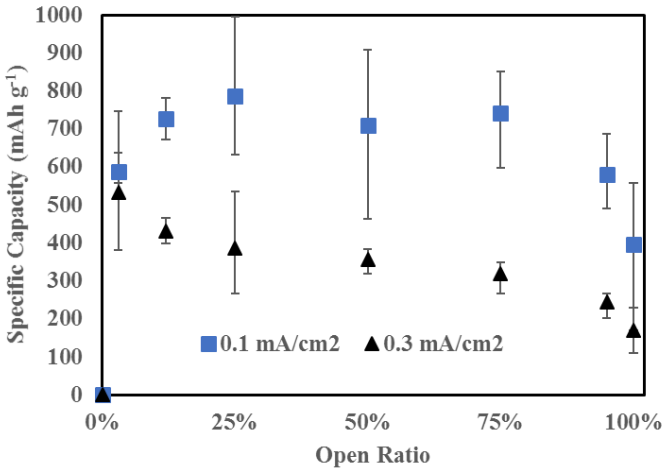

Fig. 2-4. Summary of the battery discharge specific capacity, discharged at 0.1 and 0.3 mA/cm^2 at different open ratios.

and the polarization curves at the best performance are compared in this figure. As expected, the discharge capacity was negligible (less than 1 mAh/g_{carbon}) at 0% open ratio (titanium chip with no hole) and was not presented in this figure. As the open ratio increased from 0% to 3%, 12% and then 25%, the discharge capacity increased from 1 to 586, 726 and then 994 mAh/g_{carbon} respectively. As the open ratio further increased to 50% and then 75%, the discharge capacity slightly decreased to 708 and 850 mAh/g_{carbon}, respectively. An additional increase in the open ratio resulted in a sudden drop in discharge capacity. As the open ratio increased to 100%, the discharge capacity diminished to 557 mAh/g_{carbon}, which was even slightly lower than the capacity at 3% open ratio. To clarify the battery performance versus the open ratio, a summary of the average discharge specific capacity of the batteries at different open ratios are presented in Fig. 2-4, where error bars indicate the maximum and minimum found in multiple trials. As can be seen, at 0.1 mA/cm^2 current density, the battery's performance improves as the open ratio increases to about 25% and then slowly decreases with further increase of open ratios. Theincreasing trend observed at low open ratios (less than 25%) is consistent with the previous study of Jiang et al. [20]. Results at high open ratios (higher than 25%), however, are different from some previous model simulations [3].

The discharge-charge performances of Li-O_2 batteries using an organic electrolyte are limited by the oxygen cathode instead of the Li anode. The low actual specific capacity, compared with the theoretical specific capacity, is partially caused by the precipitation of lithium oxides within the electrode and low diffusivity of the oxygen in the electrolyte. Oxygen supply is an important factor on battery's performance and has a direct impact on the discharge capacity [8][23]. Since increasing the open ratio of oxygen electrode directly increases the contact area between oxygen and electrode, the oxygen supply is greater. As a result, the discharge and charge capacity of the battery are expected to improve with the increase of the open ratio. This concept has been theoretically examined by Li et al. [3] through a modeling

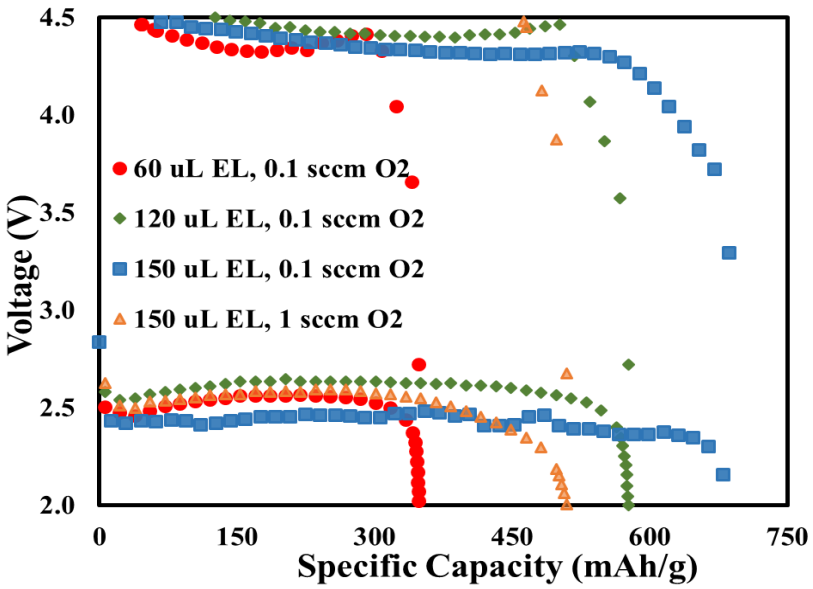

Fig. 2-5. Discharge specific capacity vs voltage, discharged at 0.1 mA/cm2, 95% open ratio, with various amount of electrolyte, 60 µL, 120 µL and 150 µL, and various oxygen flow rate, 0.1 sccm and 1 sccm.

study, which showed that increasing the open ratio would increase the discharge capacity. It should be noted that in all these studies, the electrode was assumed to be fully saturated with electrolyte during discharge and charge process and oxygen only diffused through the liquid electrolyte (no gas phase in the electrode).

In this experiment, enough electrolyte was added to all batteries during the assembly process to make sure both the electrode and separator were fully saturated. However, it was observed that electrodes were dried after each discharge-charge cycle. To demonstrate the importance of the remained amount of electrolyte, various amount of electrolyte (60 µL, 90 µL and 150 µL) had been applied to the separator and electrode of a battery with 95% open ratio and discharged at 0.1 mA/cm^2 while the oxygen flow rate was set at 0.1 sccm. Results plotted in Fig. 2-5 shows that when the initial amount of electrolyte increased from 60 to 120 and then to 150 µL, the specific discharge capacity increased from 348 to 579 and 687 mAh/g_{carbon} respectively. Remaining amount of electrolyte during discharge-charge process is a function of both the initial amount of added electrolyte and electrolyte loss rate. To investigate the effect of the electrolyte loss rate, a higher oxygen flow rate of 1 sccm was used for a battery with all

other initial conditions same as the previous case with 150 µL initial amount of electrolyte. Electrolyte loss due to evaporation is proportional to the oxygen flow rate. As Fig. 2-5 shows that by increasing the oxygen flow rate from 0.1 to 1 sccm, the discharge specific capacity decreased from 687 to 509 mAh/g_{carbon} while the charge capacity decreased from 515 to 49 mAh/g_{carbon}. The sudden drop in charge capacity can be caused by reduced amount of electrolyte and incapability of lithium ions to migrate back to lithium anode during charge process. Results of this experiment indicated that the remaining amount of the electrolyte was critical and should be considered in all model simulations and experimental studies.

Electrolyte can be lost during the discharge and charge process because of evaporation [25] , anode volume change[26], wettability of electrode and packing pressure applied by adjacent parts. The remaining amount of electrolyte in the cathode at each period of time not only depends on the initial amount of electrolyte but also on the evaporation rate. Since identical electrodes and the same amount of electrolyte (150 µl) were used at the beginning of the experiments (presented in Fig. 2-3 and Fig. 2-4), the factor that made the remained amount of electrolyte different at various open ratios of the oxygen electrode, was the evaporation rate of the electrolyte. The evaporation of the electrolyte is proportional to the oxygen flow rate passing by the battery as well as the exposed surface area of the oxygen electrode. The electrolyte loss causes two counter effects on the battery performance: 1) the oxygen diffusivity through the electrode is increased due the fact that the oxygen diffusivity in the gas phase is several orders of magnitude larger than in liquid electrolyte; and 2) the oxygen reduction reaction (ORR) stops in dry pores without electrolyte due to the lack of the three-phase boundary (which requires O_2, electrolyte, and carbon). The evaporation of electrolyte moved the electrolyte-oxygen interface towards the separator. Therefore, the Li_2O_2 film generated by the ORR was less likely to block pores at the electrode-oxygen interface due to the evaporation of the electrolyte. In order to achieve the maximum discharge and charge capacity, the

electrolyte loss rate should be slow enough so most of the pore volume is utilized for the ORR but fast enough to prevent the deposited discharge product from completely blocking the oxygen diffusion pathway. As a result, when the open ratio of the electrode was relatively high (more than 25%), further increasing the open ratio resulted in fast evaporation of the electrode and decreased the discharge capacity.

Fig. 2-6 shows the first discharge and charge cycle of Li-O_2 batteries at 0.3 mA/cm^2 at different open ratios. At this current density, the best discharge and charge performance were achieved at 3% open ratio. As the open ratio increased from 3% to 100%, the discharge capacity decreased from 747.23 mAh/g_{carbon} to 228.09 mAh/g_{carbon}. Although a similar trend of the capacity change with the open ratio was observed at 0.3 mA/cm^2, both the discharge and charge capacities significantly decreased as the current density increased from 0.1 mA/cm^2 to 0.3 mA/cm^2. This is in agreement with the known issue of limited oxygen diffusivity in Li-O_2 batteries. As the discharge current increased, the rate of ORR increased proportionally, but the oxygen diffusivity remains unchanged. Therefore, the rate of oxygen consumption is higher than the rate of oxygen transport at higher current densities. The lack of oxygen in electrode's interior pores stalls the ORR in these sites and as a result, most of the ORR takes place at the

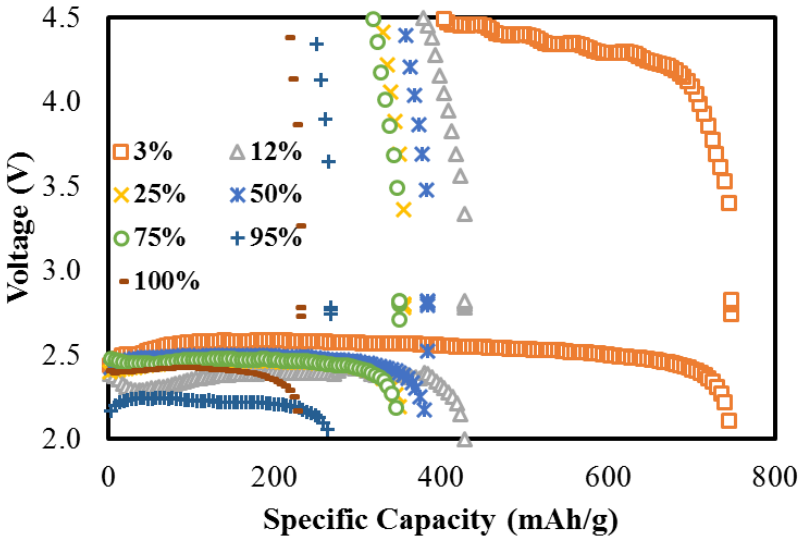

Fig. 2-6. The first discharge charge cycles of Li-O_2 batteries at 0.3 mA/cm^2 current density with 1 M electrolyte at different oxygen diffuser (current collector) open ratios

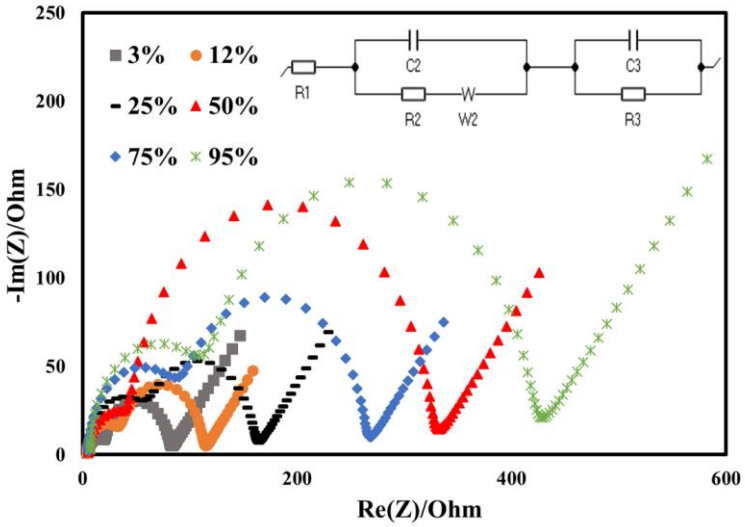

Fig. 2-7. Nyquist plots of the battery at OCV, at open ratios of 3%, 12%, 25%, 50%, 75% and 95%. The point are simulated data obtained using the equivalent circuit showed in the figure.

electrode-oxygen interface. This would cause Li_2O_2 film formation and pore blockage at the electrode-oxygen interface, which further reduces the O_2 diffusion to the interior pores. Fig. 2-4 shows the average (of repeated tests) specific discharge capacity of the battery at 0.3 mA/cm^2 at various open ratios. The trend is similar to the previous case where the batteries discharged at 0.1 mA/cm^2, while the specific discharge capacities are smaller at 0.3 mA/cm^2.

Electrical resistance is another factor that could affect the battery performance adversely. EIS was used to determine the impedance properties of the Li-O_2 battery at different open ratios at the open circuit voltage (OCV). Fig. 2-7 shows the Nyquist plots of fitted data using the equivalent circuit. The equivalent circuit includes an ohmic resistance (R_1), which considers all the electronic resistance of the electrodes, current collectors, and electrolyte, as well as the contact resistance between these components [27]. This resistance is determined as the intercept of the small semicircle by real axis at high frequencies. R_2 and R_3 are due to charge transfer resistance and mass transfer resistance at the two electrodes. These resistances are determined by the radius of the two semicircles. The diagonal line at low frequencies represents the Warburg impedance (W_2), which is due to the diffusion impedance of the oxidant and reductant.

Table 2-I. Equivalent circuit parameters of the battery at open ratios of 3%, 12%, 25%, 50%, 75% and 95%.

Open ratio	R_1 (Ohm)	C_2 (F)	R_2 (Ohm)	W_2 (Ohm.s$^{-1/2}$)	C_3 (F)	R_3 (Ohm)	OCV (V)
3%	3.97	2.08E-06	59.46	53.15	1.60E-07	16.21	3.35
12%	3.93	2.41E-06	77.02	37.68	1.89E-07	30.30	2.92
25%	5.11	1.46E-06	99.93	55.02	1.29E-07	54.62	3.41
50%	5.80	8.48E-07	280.17	81.27	1.13E-07	37.05	3.26
75%	5.12	1.39E-06	170.93	59.27	9.76E-08	85.80	3.17
95%	7.02	8.19E-07	300.13	132.54	5.88E-08	108.55	2.83

A double layer capacitance is formed when a non-conducting media separates two conducting electrodes, which is represented as C_2 and C_3 in this figure. The parameters obtained from the equivalent circuit in this figure are listed in Table 2-I. The ohmic resistance, R_1, increased from 3.97 Ω to 7.02 Ω when the open ratio increased from 3% to 95%. The increase of the ohmic resistance with an increasing open ratio was caused by the decrease of the contact surface area between oxygen diffuser (current collector) and also due to an uneven pressure distribution. Due to small specific current densities of the experiment (0.1 and 0.3 mA/cm^2), however, the increase of R_1 did not have a significant influence on the battery performance. The over-potential (calculated by multiplying R_1 with the current density) caused

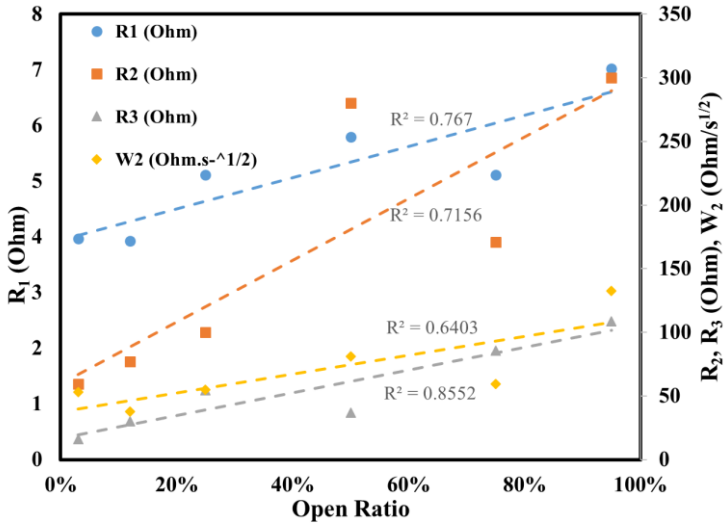

Fig. 2-8. Impedance properties of the battery vs. the electrode open ratio.

by the ohmic resistance led to less than 2 mV change in voltage plateau of the battery. As shown in Fig. 2-8, all the battery impedances, R_1, R_2, R_3, and W_2, have an increasing trend with the increase of the open ratio. Higher values of R_2 and R_3 indicate more sluggish charge and mass transfer. This is consistent with the experimental results of discharge performance versus open ratio.

Conclusions

In this chapter, discharge and charge capacities of Li-O_2 batteries with different open ratios of the oxygen electrode were experimentally measured at current densities of 0.1 and 0.3 mA/cm^2. For batteries discharged at 0.1 mA/cm^2, as the open ratio increased from 0% to 25%, the specific discharge capacity increased from less than 1 mAh/g_{carbon} to 995 mAh/g_{carbon}. As the open ratio further increased, discharge capacity slowly decreased to 397 mAh/g_{carbon} at 100% open ratio. The experiments had a similar trend at the discharge current density of 0.3 mA/cm^2, but the maximum discharge capacity was obtained at a much lower open ratio of 3% among tested open ratios. Discharge capacity was decreased from 747 to 228 mAh/g_{carbon}, when the open ratio increased from 3% to 100%. Although increasing the cathode open ratio leads to a sufficient oxygen supply within the electrode, it increases the evaporation loss of the electrolyte, as well as the contact resistance of the battery. The impact of the contact resistance increase was negligible considering the very low discharge current. As the open ratio was increased, the increase of the electrolyte evaporation rate had a significant impact on the battery performance. The balance between availability of oxygen and the utilization rate of the electrode, caused by the evaporation of the electrolyte, resulted in a peak discharge capacity at the open ratio of 25% and 3% at 0.1 and 0.3 mA/cm^2, respectively. The results indicated that the open ratio should be optimized based on the discharge current to maximize the battery specific capacity. Our study on this subject is required to quantify the evaporation rate and its significance on battery operation and on the methods to control this rate.

References

[1] J. Lu, L. Li, J.-B. Park, Y.-K. Sun, F. Wu, K. Amine, Aprotic and aqueous Li-O2 batteries, Chemical Reviews. 114 (2014) 5611–5640.

[2] P.G. Bruce, S.A. Freunberger, L.J. Hardwick, J.-M. Tarascon, Li-O2 and Li-S batteries with high energy storage, Nature Materials. 11 (2012) 19–29.

[3] X. Li, A. Faghri, Optimization of the cathode structure of lithium-air batteries based on a two-dimensional, transient, non-isothermal model, Journal of The Electrochemical Society. 159 (2012) A1747–A1754.

[4] J. Yuan, J.-S. Yu, B. Sundén, Review on mechanisms and continuum models of multi-phase transport phenomena in porous structures of non-aqueous Li-Air batteries, Journal of Power Sources. 278 (2015) 352–369.

[5] K. Abraham, Z. Jiang, A polymer electrolyte-based rechargeable lithium/oxygen battery, Journal of The Electrochemical Society. 143 (1996) 1–5.

[6] G. Girishkumar, B. McCloskey, A. Luntz, S. Swanson, W. Wilcke, Lithium- air battery: promise and challenges, The Journal of Physical Chemistry Letters. 1 (2010) 2193–2203.

[7] J. Read, Characterization of the lithium/oxygen organic electrolyte battery, Journal of The Electrochemical Society. 149 (2002) A1190–A1195.

[8] J. Read, K. Mutolo, M. Ervin, W. Behl, J. Wolfenstine, A. Driedger, et al., Oxygen transport properties of organic electrolytes and performance of lithium/oxygen battery, Journal of The Electrochemical Society. 150 (2003) A1351–A1356.

[9] K. Xu, Nonaqueous liquid electrolytes for lithium-based rechargeable batteries, Chemical Reviews. 104 (2004) 4303–4418.

[10] G.M. Veith, J. Nanda, L.H. Delmau, N.J. Dudney, Influence of lithium salts on the discharge chemistry of Li-air cells, The Journal of Physical Chemistry Letters. 3 (2012) 1242–1247.

[11] P. Du, J. Lu, K.C. Lau, X. Luo, J. Bareño, X. Zhang, et al., Compatibility of lithium salts with solvent of the non-aqueous electrolyte in Li-O 2 batteries, Physical Chemistry Chemical Physics. 15 (2013) 5572–5581.

[12] G.A. Elia, J.-B. Park, Y.-K. Sun, B. Scrosati, J. Hassoun, Role of the Lithium Salt in the Performance of Lithium-Oxygen Batteries: A Comparative Study, ChemElectroChem. 1 (2014) 47–50.

[13] C.O. Laoire, S. Mukerjee, K. Abraham, E.J. Plichta, M.A. Hendrickson, Influence of nonaqueous solvents on the electrochemistry of oxygen in the rechargeable lithium- air battery, The Journal of Physical Chemistry C. 114 (2010) 9178–9186.

[14] W. Xu, J. Xiao, D. Wang, J. Zhang, J.-G. Zhang, Effects of nonaqueous electrolytes on the performance of lithium/air batteries, Journal of The Electrochemical Society. 157 (2010) A219–A224.

[15] W. Xu, J. Xiao, J. Zhang, D. Wang, J.-G. Zhang, Optimization of nonaqueous electrolytes for primary lithium/air batteries operated in ambient environment, Journal of the Electrochemical Society. 156 (2009) A773–A779.

[16] E.J. Nemanick, R.P. Hickey, The effects of O 2 pressure on Li-O 2 secondary battery discharge capacity and rate capability, Journal of Power Sources. 252 (2014) 248–251.

[17] X. Yang, Y. Xia, The effect of oxygen pressures on the electrochemical profile of lithium/oxygen battery, Journal of Solid State Electrochemistry. 14 (2010) 109–114.

[18] P. Tan, W. Shyy, L. An, Z. Wei, T. Zhao, A gradient porous cathode for non-aqueous lithium-air batteries leading to a high capacity, Electrochemistry Communications. 46 (2014) 111–114.

[19] F. Mohazabrad, F. Wang, X. Li, Experimental Studies of Salt Concentration in Electrolyte on the Performance of Li-O2 Batteries at Various Current Densities, Journal of The Electrochemical Society. 163 (2016) A2623–A2627.

[20] J. Jiang, H. Deng, X. Li, S. Tong, P. He, H. Zhou, Research on Effective Oxygen Window Influencing the Capacity of Li-O2 Batteries, ACS Applied Materials \& Interfaces. 8 (2016) 10375–10382.

[21] X. Li, J. Huang, A. Faghri, Modeling study of a Li-O 2 battery with an active cathode, (2015).

[22] F. Mohazabrad, X. Li, Influence of Oxygen Electrode Open Ratio and Electrolyte Evaporation on the Performance of Li-O_2 Batteries, Modeling Study, Journal of Power Source, (2013), Under Review.

[23] I. Kowalczk, J. Read, M. Salomon, Li-air batteries: A classic example of limitations owing to solubilities, Pure and Applied Chemistry. 79 (2007) 851–860.

[24] S.S. Zhang, D. Foster, J. Read, Discharge characteristic of a non-aqueous electrolyte Li/O 2 battery, Journal of Power Sources. 195 (2010) 1235–1240.

[25] J. Huang, A. Faghri, Analysis of electrolyte level change in a lithium air battery, Journal of Power Sources. 307 (2016) 45–55.

[26] K. Yoo, S. Banerjee, P. Dutta, Modeling of volume change phenomena in a Li-air battery, Journal of Power Sources. 258 (2014) 340–350.

[27] C. Laoire, S. Mukerjee, E.J. Plichta, M.A. Hendrickson, K. Abraham, Rechargeable lithium/TEGDME-LiPF6/ O2 battery, Journal of The Electrochemical Society. 158 (2011) A302–A308.

Chapter 3. Influence of Oxygen Electrode Open Ratio and Electrolyte Evaporation on the Performance of Li-O_2 Batteries, Modeling Study

In this chapter, a two-dimensional transient model has been developed to study the influence of the cathode electrode open ratio on the mass transfer properties of the Li-O_2 battery. The open ratio is defined as the ratio of the surface area of the cathode/oxygen opening to the surface area of the cathode electrode. The effect of electrolyte level change in combination with cathode open ratio was investigated and accuracy of the results had been verified by our experiments. Modeling results indicate that when the electrolyte level remained constant (cathode electrode was saturated with electrolyte), the oxygen concentration was the limiting factor on the battery discharge capacity. The vast majority of the discharge products (Li_2O_2) deposited at the electrode/oxygen interface further reduce the oxygen flux to the interior pores of the electrode. The discharge capacity increased significantly from 99.7 to 1387 mAh g^{-1}, when the open ratio increased from 25% to 100%. This model also simulated the scenario in which the electrolyte level changes due to the volume change of the solid and electrolyte evaporation (proportional to cathode open ratio) was considered. The modeling results showed that the oxygen transfer within the electrode partially filled with the electrolyte was remarkably improved since the oxygen diffusivity in the gas phase is several orders of magnitude higher than that in the electrolyte. As a result, more pores were utilized for the oxygen reduction reaction (ORR). When the evaporation of the electrolyte was considered, the discharge capacity decreased from 842 to 517 mAh g^{-1} at 0.1 mAh cm^{-2} with 0.1 sccm oxygen flow rate when the open ratio increased from 25% to 100%.

3-1. Introduction

The Li-O_2 battery is a promising energy storage device with extremely high theoretical specific energy due to the high energy capacity of lithium metal and unlimited availability of oxygen as the cathode active material in the ambient air. This technology has attracted more

research in recent years due to the increasing demand for a high capacity power supply system for portable electronic devices and electric vehicles. Decreasing resources of fossil fuels, increasing fossil fuels prices, and extensive greenhouse gas emissions and global climate change associated with fossil fuel usage are among the motives for this research. A high capacity energy storage system can also be used to balance the power grid system and renewable energies peak production and demand. Lithium metal is highly reactive and while this property is favorable for the main discharge and charge reactions, its severe reaction with water vapor from air with electrolyte and salt species can result in some safety and irreversibility issues. Although the Li-O_2 oxygen was first introduced in the 1970s, it was not accepted as a possible energy storage system until 1996 when Abraham and Jiang [1] proposed a rechargeable Li-O_2 battery that used organic electrolyte as the solvent. Organic electrolytes are mainly used because of a higher Li-O_2 battery capacity and also because of the reduction of lithium anode corrosion from the lack of water content in these electrolytes in comparison with aqueous electrolytes. However, the full potential of the Li-O_2 battery is not yet realized, mainly because of the limited oxygen diffusivity and insolubility of the discharge products in an organic electrolyte [2].

Among all the chemical and electrochemical reactions involved in Li-O_2 battery, the two-electron reaction presented in Eq. 1 is widely accepted when an organic electrolyte is used [3].

$$2\mathrm{Li}^+ + 2\mathrm{e}^- + \mathrm{O}_2 \leftrightarrows (\mathrm{Li}_2\mathrm{O}_2)_\mathrm{S} \quad \mathrm{E}_{rev} = 2.96\ \mathrm{V} \tag{1}$$

Due to the importance of oxygen supply in the oxygen electrode, we have recently experimentally investigated the influence of the cathode electrode open ratio on the performance of Li-O_2 battery at various discharge current densities [4]. Electrolyte was prepared with 1M concentration of bis(trifluoromethane)sulfonamide lithium salt (LiTFSI) dissolved in tetraethylene glycol dimethyl ether (TEGDME). A wide range of open ratios, 3%

to 100%, were selected for this study. The first discharge-charge cycle specific capacities were measured at current densities of 0.1 and 0.3 mA/cm^2. At the current density of 0.1 mA/cm^2, the maximum discharge capacity was achieved at 25% open ratio among the selected open ratios for this experiment. As the open ratio increased from 25% to 100%, the specific discharge capacity decreased from 995 to 397 mAh/g_{carbon}. The maximum discharge capacity at 0.3 mA/cm^2 was obtained at much lower open ratio of 3% among tested open ratios. Discharge capacity decreased from 747 to 228 mAh/g_{carbon} when the open ratio increased from 3% to 100%. Fast evaporation of electrolyte at relatively high open ratios was one of the main reasons for the decrease of the discharge capacity with increasing open ratio. Volume change of the electrolyte is caused by evaporation, volume change of the solid, and leakage during the discharging and charging process. This volume change can significantly impact the oxygen supply, as well as the ionic conductivity within the oxygen electrode. Additional investigations are needed to understand the quantitative impact of the volume change of electrolyte (especially by evaporation) on the battery performance.

Modeling studies support experiments and allow us to obtain a better understanding of the coupling between the multi-phase mass transfer in the porous electrode and electrochemical reactions. Many models, based on analytical methods or numerical simulations, have been developed in recent years to study the multi-phase mass transfer within the porous electrode of Li-O_2 batteries.

Li and Faghri [5] developed a transient two-dimensional (2-D) model to study the effects of discharge current, cathode porosity distribution, cathode thickness, and cathode open ratio. Modeling results showed that a better specific capacity can be realized at a lower current density with thinner cathodes and higher cathode open ratios. The modeling results indicated that the specific capacity increased from 133 to 529 mAh g^{-1} when the cathode open ratio increased from 50% to 100%. It is also showed that a better specific capacity can be achieved

by redesigning the cathode porosity distribution to have higher porosity at the air side and lower porosity at the anode side. All these results are obtained with the assumption that the cathode electrode is fully saturated with electrolyte all the time. Therefore, the increase of the discharge capacity resulted from the enhanced mass transfer of oxygen in the cathode. In 2015, Ye et al. [6] developed an analytical model to study energy loss associated with diffusion of oxygen. It was concluded that a thin cathode with a large porosity was more favorable to increase the oxygen diffusion. A wetted diffusion model was proposed to show that a flooded electrode impacts the battery performance negatively and a partially wetted electrode was more desirable since it promoted the diffusion in the gas phase and decreased the concentration over-potential.

A numerical method was introduced by Yoo et al. [7] to study the significance of the volume change of the Li anode corresponding to the performance of the battery. For the discharge and charge reactions, Li ions travel between the anode and cathode. In this study, the volume change of the anode appeared as a gap between the separator and Li anode. During discharge, the gap increased due to the transport of Li^+ to the cathode and the porosity of the cathode decreased due to the formation and deposition of Li_2O_2 on the cathode pores. This means that the available space for the electrolyte (that initially filled the pores of the cathode and separator) changes with time. Their results indicated that the available space in the oxygen electrode decreased during discharge due to the generation of insoluble Li_2O_2, which caused the leakage of electrolyte. This leakage was proportional to the current density and specific capacity. At a current density of 1 mA/m^2, 2.15% of the electrolyte leaked out at the specific capacity of 650 mAh/g.

Huang and Faghri [8] developed a 2-D model that captured electrolyte evaporation in addition to the volume change of the solid phase. The evaporation rate was a function of the partial pressure of solvent vapor and air chamber size. The volume change of the solid phase was related to the specific volume difference between the Li metal and Li_2O_2. A highly volatile

electrolyte, DMF, and a less volatile electrolyte, TEGDME, were compared in this study. It showed that the evaporation rate of was the highest at the beginning of discharge and decreased once the partial pressure of the solvent in air chamber reached the saturation level. This volume change had a significant influence on the Li_2O_2 distribution and specific discharge capacity. The reaction sites with the fastest reaction rate moved deep into the electrode as the interface between the electrolyte and air moved away from the air inlet. The moving of the electrolyte-air interface resulted in a better utilization of the cathode electrode since the oxygen supply increased. The specific discharge capacity of the battery increased by 22.5% and 14.9% with DMF and TEGDME electrolytes, respectively. It was also demonstrated that the size of the air chamber size was critical in battery performance. The discharge capacity was increased by 72% simply by increasing the air chamber radius from 5 cm to 15 cm. It should be noted that only one open ratio, 100%, was considered in this study and the battery was connected with a limited size air chamber. However, a real Li-O_2 battery operates in the ambient with an unlimited amount of air, hence the partial pressure of the solvent in ambient would never reach the saturation level. Under ambient conditions, an oxygen selective membrane should be added between cathode and air entrance opening to prevent water vapor from entering the battery that oxidizes the Li anode and causes side reactions in the oxygen electrode. Meanwhile, this oxygen-selection membrane has a significant impact on the evaporation rate of the solvent [9].

Recently, Jiang et al. [10] conducted experimental research on the effects of the oxygen window on the capacity of Li-O_2 batteries. In this work, a single hole with different diameters was machined on the oxygen side of the coin-cell battery as the oxygen window. The battery consisted of a homemade electrode, a glass fiber separator, a Li anode, and 50 µL of $LiCF_3SO_3$-TEGDME (1:4 molar ratio) as the organic electrolyte solution. All batteries were tested in an oxygen-filled glass chamber at 25 ^oC and 1 atm during the discharge-charge process. The first discharge-charge cycle of the Li-O_2 batteries at a current of 0.1 mA showed

that battery capacity increases linearly with the size of the oxygen window. It should be noted that in this work, the electrode was prepared by adding a gas diffusion layer on a catalytic layer with 12 mm diameter (113.1 mm^2) and the size of the biggest oxygen window in this work was 22 mm^2. Therefore, the maximum open ratio (ratio between oxygen window area to the total electrode surface area was calculated to be about 19.5%. In this work, we have developed a two-dimensional model to study the effect of the open ratio (between 25% and 100%) of the oxygen electrode on Li-O_2 battery performance. A constant flow of oxygen (0.1 sccm) through the cathode air channel was considered to better simulate the oxygen supply condition in practical battery applications. This novel model that considers the evaporation of electrolyte can accurately predict discharge capacities at various open ratios observed by our experiments (the experimental results are published in a separate paper) [15].

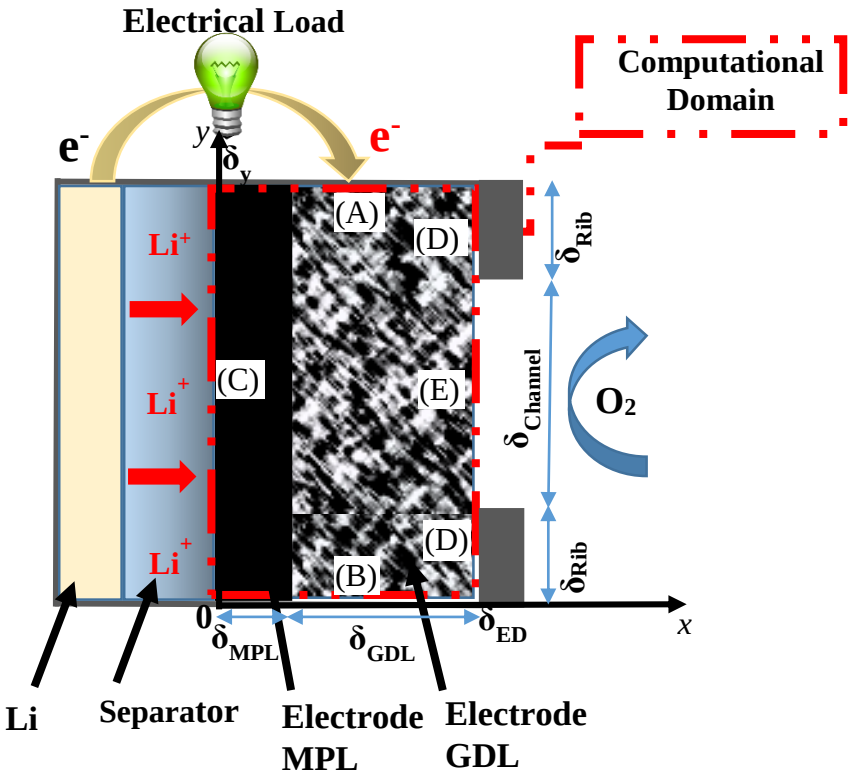

Fig. 3-1. Computational domain of a Li-O_2 battery using LiTFSI/TEGDME electrolyte and carbon cloth GDL with MPL as the electrode.

3-2. Mathematical Model

In this study, a two-dimensional model was developed to study the transient discharge process in the oxygen electrode of a Li-O_2 battery. This model solved two-dimensional mass transfer, the energy equation, and electrochemical performance simultaneously inside the cathode oxygen electrode, as illustrated by the dashed line in Fig. 3-1. The governing equations of the concentrations of oxygen and lithium ions are considered in the local reaction rate and in the amount of the solid Li_2O_2 deposited on the cathode surface. In addition, physical properties of the electrode, such as diffusivity, porosity, tortuosity, active area of the electrode, etc. were updated based on the amount of Li_2O_2 generated at each time step. The following assumptions were adopted in order to simplify the analysis and focus on the main parameters and phenomena within the subject of this study:

1. The discharge over-potential at the Li anode is negligible [23].
2. The electrode is fully filled with the electrolyte at the beginning of discharge and lithium ion only transfer in the liquid electrolyte [5].
3. The convection effect is negligible and oxygen and lithium ion only transfer by diffusion [5].
4. The Li_2O_2 particles are much smaller than the electrode and Li_2O_2 is assumed to deposit on the electrode surface as a smooth film [11].
5. Due to the high thermal conductivity of the battery frame and lithium metal, it is assumed that all these surfaces stay at the surrounding temperature [5].

The concentrations of lithium ion and dissolved oxygen in the electrolyte are solved by: [12]

$$\frac{\partial(\varepsilon\rho_{\mathrm{EL}}\omega_{\mathrm{Li^+}})}{\partial \mathrm{t}} = \nabla.\left(\rho_{\mathrm{EL}} D_{\mathrm{Li^+}}^{\mathrm{eff}} \nabla\omega_{\mathrm{Li^+}}\right) + \dot{m}_{\mathrm{Li^+}} \tag{2}$$

$$\frac{\partial(\varepsilon\rho_{\mathrm{EL}}\omega_{\mathrm{O_2}})}{\partial \mathrm{t}} = \nabla.\left(\rho_{\mathrm{EL}} D_{\mathrm{O_2}}^{\mathrm{eff}} \nabla\omega_{\mathrm{O_2}}\right) + \dot{m}_{\mathrm{O_2}} \tag{3}$$

where ω is the mass concentration, ε the porosity of the electrode, ρ_{EL} the density of the electrolyte, and D_i^{eff} the effective diffusivity. The Bruggeman relation is used to calculate the effective diffusivity of the species in the electrolyte. Effective diffusivity is determined by the initial diffusivity, D_i, and porosity of the electrode, ε, and tortuosity of the electrode, τ:

$$D_i^{eff} = D_i \varepsilon^{\tau} \tag{4}$$

where the tortuosity is a function of porosity: $\tau(\varepsilon) = 1 - 0.77 \ln(\varepsilon)$ (5)

Similar to the commercial electrodes used in our previous experimental study[4], the electrode here also consists of a gas diffusional layer (GDL), made from carbon cloth, and a micro porous layer (MPL), made from carbon powders. The computational domain was composed of two regions to represent the GDL and MPL, respectively. The GDL region was considered as a porous medium with the porosity of 80% and the average pore size of 10 μm. While the MPL region was treated as a porous medium with the porosity of 65% and the average pore size of 125 nm[13]. The consumption (and generation) rates of species Li^+ and O_2 in eq. 2 and 3 are:

$$\dot{m}_{Li^+} = -\frac{R_{ORR}}{F} M_{Li} \quad \left[\frac{g}{m^3.s}\right] \tag{6}$$

$$\dot{m}_{O_2} = -\frac{R_{ORR}}{2F} M_{O_2} \quad \left[\frac{g}{m^3.s}\right] \tag{7}$$

where R_{ORR} is the rate of oxygen reduction reaction (ORR), and F is the Faradic constant, 96,487 C mol^{-1}. The rate of ORR is different at each computational volume in the cathode oxygen electrode and changes with time. The ORR depends on concentrations of the lithium ion and oxygen, ω_{Li^+} and ω_{O_2}, temperature, T, the active surface area of the electrode per volume, A_{ED}, standard rate constant, k_{ORR}, and the over-potential, η, by the following equation: [5]

$$R_{ORR} = \left(\frac{\omega_{Li^+}}{\omega_{Li^+}^{ref}}\right).\left(\frac{\omega_{O_2}}{\omega_{O_2}^{ref}}\right).k_{ORR}.A_{ED}.\exp.\left(\frac{\alpha_{ORR}F}{RT}\eta\right) \tag{8}$$

The temperature distributions are calculated by solving the following energy balance equation: [12]

$$\rho C_P \frac{\partial(T)}{\partial \mathrm{t}} = \nabla.(K_\mathrm{T} \nabla T) + \dot{m}_\mathrm{T} \tag{9}$$

where the value of specific heat, ρC_P, and the effective thermal conductivity, K_T, are related to volume fraction and properties of the electrode, Li_2O_2 precipitate, and electrolyte. The energy source term, $\dot{m}_T$ is related to the reaction over-potential, η, and Rate of ORR, and can be calculated by:

$$\dot{m}_T = R_\mathrm{ORR}.\eta \quad \left[\frac{\mathrm{W}}{\mathrm{m}^3}\right] \tag{10}$$

In this model, the effect of deposition of Li_2O_2 on the cathode surface area was considered by the variation of standard rate constant, k_ORR. This method was fully described in our previous study [14], which assumed that this value decreased as the Li_2O_2 deposits on the surface of the electrode. It has been determined that the standard rate constant, k_ORR, reduced in two distinct steps. These steps were correlated to the quantity of discharged electricity per surface area of the electrode, q, and is the ratio of the accumulated local reaction rate and surface area of the electrode per volume $A_\mathrm{eff}/V_\mathrm{ED}$: [14]

$$q\ (t) = \frac{\int R_\mathrm{ORR}.\mathrm{dt}}{A_\mathrm{eff}/V_\mathrm{ED}} \tag{11}$$

where A_eff is the effective surface area of the electrode per volume and it changes due to the evolution of the pores.

Experimental results showed that in the first step, the standard rate constant reduces linearly by one order of magnitude when a single monolayer of the Li_2O_2 covered the electrode active surface area. The amount of Li_2O_2 was equivalent to a very small quantity of discharge (~7 C/m^2) on a glassy carbon electrode [15]. Further deposition of Li_2O_2 on the electrode passivated the electrode and empirical relations were derived based on experimental data. The change of

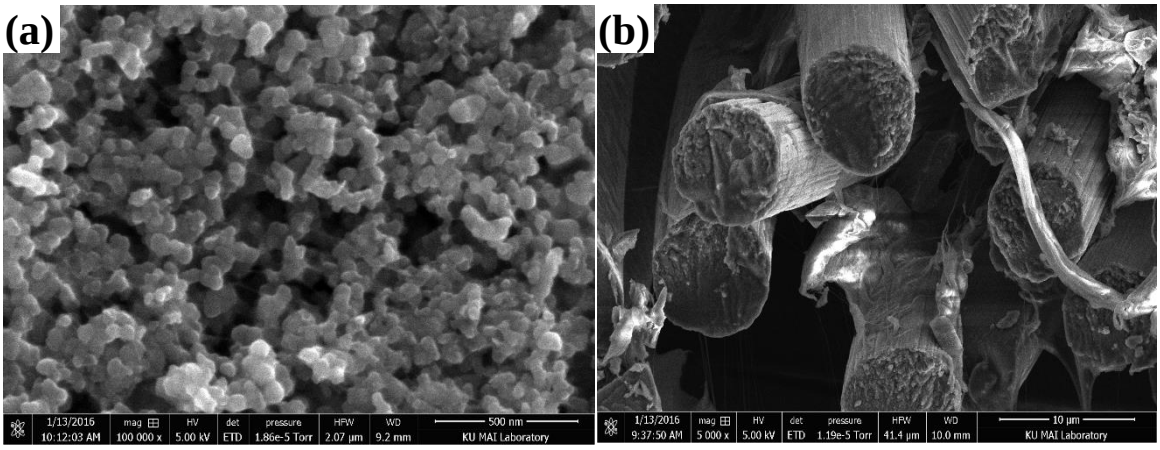

Fig. 3-2. SEM image of carbon electrode components: (a) MPL; (b) GDL.

the standard rate constant at the room temperature with the amount of Li_2O_2 deposition was described by the following equation [14]:

$$k_{\mathrm{ORR}}(293\ K) = \begin{cases} i_0 \cdot \frac{A_{\mathrm{eff}}}{V_{\mathrm{ED}}} \cdot \left(1 - 0.9\ \cdot \frac{q}{7}\right) & \text{if } q \le 7\ (\mathrm{C/m^2}) \\ 1.5245\ i_0 \cdot \frac{A_{\mathrm{eff}}}{V_{\mathrm{ED}}} \cdot 10^{-.02616q} & \text{if } q > 7\ (\mathrm{C/m^2}) \end{cases} \tag{12}$$

The standard rate constant, k_{ORR}, at other temperatures can be calculated by the following function: [14]

$$k_{\mathrm{ORR}}(T) = k_{\mathrm{ORR}}(293\ \mathrm{K}).\exp\left[\frac{E_{\mathrm{ORR}}}{R}\left(\frac{1}{295} - \frac{1}{T}\right)\right] \tag{13}$$

where E_{ORR} is the activation energy of the ORR which is approximated as 21 kJ mol^{-1} [16].

After the deposition of a single monolayer of the Li_2O_2 on the electrode surface, the kinetics of the reaction remains unchanged, but the rate of ORR still decreases by the reduction of the active surface area per volume, and also by the reduction of the porosity of the electrode. The diffusion coefficient decreases as the porosity decreases and it affects the concentration of dissolved oxygen and lithium ions in the electrolyte. The effective active surface area of electrode per volume, A_{ED}, was calculated by [5]:

$$\frac{A_{\mathrm{eff}}(t)}{A_{\mathrm{ED},0}} = \left(1 - \frac{\varepsilon_{\mathrm{Li_2O_2}}}{\varepsilon_0}\right)^{2/3} \tag{14}$$

where $A_{\mathrm{ED},0}$ is the effective active area of electrode per volume before discharge and $\varepsilon_{\mathrm{Li_2O_2}}$ is the local volume fraction of the Li_2O_2. The above equation was derived based on the

assumption that pores were in spherical shape in micro porous layer of the electrode and were in cylindrical shape in carbon cloth gas diffusional layer. Average diameters, d_{avg}, are estimated as 125 nm and 10 μm in the MPL and GDL, respectively, based on a previous study [13] and SEM images as presented in Fig. 3-2. Equations 15 and 16 [17] were used to calculate the active surface area for the purpose of this study:

$$(A_{\mathrm{ED},0})_{\mathrm{MPL}} = \frac{6\varepsilon_{0,\mathrm{MPL}}}{d_{0,\mathrm{MPL}}} \tag{15}$$

$$(A_{\mathrm{ED},0})_{\mathrm{GDL}} = \frac{4\varepsilon_{0,\mathrm{GDL}}}{d_{0,\mathrm{GDL}}} \tag{16}$$

At each time step, the local porosity in the cathode oxygen electrode was calculated by:

$$\varepsilon = \varepsilon_0 - \varepsilon_{\mathrm{Li_2O_2}} \tag{17}$$

where the local volume fraction of the Li_2O_2, $\varepsilon_{\mathrm{Li_2O_2}}$ was calculated based on the amount of accumulated Li_2O_2[5]:

$$\varepsilon_{\mathrm{Li_2O_2}} = \frac{\int R_{\mathrm{ORR}}.\mathrm{dt}}{2\mathrm{F}} \frac{M_{\mathrm{Li_2O_2}}}{\rho_{\mathrm{Li_2O_2}}} \tag{18}$$

The production rate of Li_2O_2 was calculated from the reaction rate of the ORR:

$$\dot{m}_{\mathrm{Li_2O_2}} = \frac{R_{\mathrm{ORR}}}{2F} M_{\mathrm{Li_2O_2}} \quad \left[\frac{\mathrm{g}}{\mathrm{m^3.s}}\right] \tag{19}$$

The discharge current in this model was calculated by integrating the ORR rates over the whole computational domain:

$$I = \int_{\mathrm{Electrode}} R_{\mathrm{ORR}} \cdot dx \cdot dy \tag{2}$$

The porous oxygen electrode has a complex microscopic structure with heterogeneous pore-scale physical and chemical properties, such as the wettability, catalytic activity, and pore distribution. Therefore, electrochemical reactions, oxygen diffusivity, and electrolyte evaporation are non-uniform throughout the electrode. As was stated in previous research by Li et al. [17], a macroscopic model that can consider all three phases (solid, electrolyte, and gas) is necessary to simulate transport phenomena in real electrodes that are partially filled with the electrolyte. The model developed in this study considered all three phases with the

simplification of a uniform velocity change rate of the electrolyte level, $\vec{V}_{\mathrm{EL}}$, due to evaporation of the electrolyte and volume change of the solid phase (including the Li metal and the discharge products):

$$\vec{V}_{\mathrm{EL}} = -\left(\vec{V}_{\mathrm{vol}} + \vec{V}_{\mathrm{evap}}\right) \tag{21}$$

where $\vec{V}_{\mathrm{vol}}$ is the velocity due to the volume change of the solid phase and $\vec{V}_{\mathrm{evap}}$ is the velocity due to evaporation.

Two moles of light weight Li metal is consumed to produce one mole of denser discharge product, Li_2O_2, during discharge, which decreases the volume of the solid phase [8]. It was assumed that the electrolyte always filled the gap between the separator and Li anode, therefore, the volume change of the solid phase resulted in the change of electrolyte level at the electrode-O_2 interface. This phenomenon is explained thoroughly and formulated in a previous study [8]:

$$\vec{V}_{\mathrm{vol}} = \frac{I}{\varepsilon_{\mathrm{avg}} \cdot \mathrm{F}} \left(\frac{M_{\mathrm{Li}}}{\rho_{\mathrm{Li}}} - \frac{M_{\mathrm{Li_2O_2}}}{2\rho_{\mathrm{Li_2O_2}}} \right) \tag{22}$$

where $\varepsilon_{\mathrm{avg}}$, is the average porosity of the electrode.

The evaporation rate of electrolyte in an ambient operated Li-O_2 battery depends on the properties of the electrode protective layer or oxygen selective membrane, electrolyte vapor pressure, oxygen pressure, and the oxygen flow rate. In this study, an O_2 flow rate of 0.1 sccm (similar to our experimental study) over the electrode surface area was assumed. The ideal gas law was used to determine the concentration of the solvent vapor in the oxygen flow and the corresponding interface velocity due to evaporation:

$$\vec{V}_{\mathrm{evap}} = \frac{P_{\mathrm{EL}}}{P_{\mathrm{O_2}}} \cdot \frac{M_{\mathrm{EL}}}{M_{\mathrm{O_2}}} \cdot \frac{\rho_{\mathrm{O_2}}}{\rho_{\mathrm{EL}}} \cdot \frac{\dot{V}_{\mathrm{O_2}}}{\varepsilon \cdot A_{\mathrm{Electrode}}} \tag{23}$$

where P_{EL} is the solvent vapor pressure, $P_{\mathrm{O_2}}$ is the oxygen pressure (10 kPa gauge pressure or 111325 absolute pressure for this study), $M_{\mathrm{EL}}$is the molecular weight of the electrolyte, $\dot{V}_{\mathrm{O_2}}$is the volume flow rate of the oxygen, and $A_{\mathrm{Electrode}}$ is the surface area of the electrode. The

evaporation rates in an electrode with different open ratios were calculated by multiplying the above evaporation rate (of an electrode fully exposed to the oxygen flow) with the open ratio.

At each time step, the over-potential was calculated to achieve the set discharge current and the cell voltage was determined by the following equation [14]:

$$V = E_0 - \eta_{\mathrm{C}} - \eta_{\mathrm{ohm.Li_2O_2}} - I \times \left(\frac{\delta_{\mathrm{ED}}}{\sigma_{\mathrm{EL}}}\right) \tag{24}$$

where E_0 is the thermodynamic equilibrium voltage, δ_{ED} is the thickness of the electrode, σ_{EL} is the conductivity of the electrolyte, and $\eta_{\mathrm{ohm.Li_2O_2}}$ is the potential drop through the deposited Li_2O_2 film as calculated by [14]:

$$\eta_{\mathrm{ohm.Li_2O_2}} = \frac{\left(\delta_{\mathrm{Li_2O_2}}/\sigma_{\mathrm{Li_2O_2}}\right)\cdot R_{\mathrm{ORR}}}{A_{\mathrm{eff}}/V_{\mathrm{ED}}} \tag{25}$$

where $\delta_{\mathrm{Li_2O_2}}$ is the thickness of Li_2O_2 film and $\sigma_{\mathrm{Li_2O_2}}$ is the electrical conductivity of this layer.

3-3. Boundary Conditions:

Boundary conditions for the computational domain are numbered in Fig. 3-1, and summarized in Table 3-I. The top and bottom are symmetric boundaries, boundary A and B are considered as adiabatic, with zero diffusion of mass and heat through these boundaries in *y*-direction.

Table 3-I. Boundary conditions

Number	Mass	Heat	Location
A &B	$\frac{\partial \omega_{\mathrm{O_2}}}{\partial \mathrm{y}} = 0$	$\frac{\partial T}{\partial \mathrm{y}} = 0$	Top and Bottom
	$\frac{\partial \omega_{\mathrm{Li^+}}}{\partial \mathrm{y}} = 0$		
C	$\frac{\partial \omega_{\mathrm{O_2}}}{\partial x} = 0$	T=298 K	Cathode/Separator
	$\omega_{\mathrm{Li^+}} = \omega_{\mathrm{Li^+}}^{\mathrm{ref}}$		
D	$\frac{\partial \omega_{\mathrm{Li^+}}}{\partial \mathrm{x}} = 0$	T=298 K	Rib/Cathode
	$\frac{\partial \omega_{\mathrm{O_2}}}{\partial \mathrm{x}} = 0$		
E	$\frac{\partial \omega_{\mathrm{Li^+}}}{\partial \mathrm{x}} = 0$	$-K_{\mathrm{T}}\frac{\partial T}{\partial \mathrm{x}} = h(T - T_\infty)$	Cathode/Air interface
	$\omega_{\mathrm{O_2}} = \omega_{\mathrm{O_2}}^{\mathrm{ref}}$		

Table 3-II. Parameters used in this model

Parameter	Symbol	Value
Initial porosity of the GDL	$\varepsilon_{0,\mathrm{GDL}}$	0.80
Initial porosity of the MPL	$\varepsilon_{0,\mathrm{MPL}}$	0.65
Room temperature	T	298 K
Molecular weight of lithium	M_{Li}	6.94 g mol^{-1}
Molecular weight of O_2	$M_{\mathrm{O_2}}$	15.99 g mol^{-1}
Molecular weight of lithium peroxide	$M_{\mathrm{Li_2O_2}}$	45.88 g mol^{-1}
Initial average pore diameter of MPL	$d_{0,\mathrm{GDL}}$	10 μm
Initial average pore diameter of MPL	$d_{0,\mathrm{MPL}}$	125 nm
Active area of the GDL per volume	$A_{0,\mathrm{GDL}}$	3.2×10^{5} m^2 m^{-3}
Active area of the MPL per volume	$A_{0,\mathrm{MPL}}$	3.12×10^{7} m^2 m^{-3}
Exchange current density	i_0^{ref}	3.11×10^{-4} [18]
Transfer coefficient of cathode	α_{ORR}	0.5 [18]
Thermodynamic equilibrium voltage	E_0	2.98
Diffusivity of oxygen in electrolyte	$D_{\mathrm{O_2}}$	2.17×10^{-6} cm^2 s^{-1} [3]
Diffusivity of Li^+ in electrolyte	$D_{\mathrm{Li^+}}$	8×10^{-7} cm^2 s^{-1} [19]
Solubility of oxygen in electrolyte		4.43×10^{-3} M cm^{-3}[3]
Reference concentration of O_2	$\omega_{\mathrm{O_2}}^{\mathrm{ref}}$	1.39×10^{-4} kg kg^{-1} [2]
Reference concentration of Li^+	$\omega_{\mathrm{Li^+}}^{\mathrm{ref}}$	6.67×10^{-3} kg kg^{-1}
Density of carbon	ρ_{C}	2.26 g cm^{-3}
Density of electrolyte	ρ_{EL}	1009 kg m^{-3}
Density of oxygen	$\rho_{\mathrm{O_2}}$	1.429 kg m^{-3}
Density of lithium	ρ_{Li}	0.534 g cm^{-3}
Density of lithium peroxide	$\rho_{\mathrm{Li_2O_2}}$	2.31 g cm^{-3}
Conductivity of the electrolyte	σ_{EL}	$0.3\times10^{-3}\ \Omega^{-1}\mathrm{cm}^{-1}$ [3]
Conductivity of the electrode	σ_{ED}	$3\ \Omega^{-1}\mathrm{cm}^{-1}$ [20]
Specific heat of electrolyte	$C_{p,\mathrm{EL}}$	2.56 J g^{-1} K^{-1} Reference 21
Specific heat of carbon	$C_{p,\mathrm{ED}}$	0.71 J g^{-1} K^{-1}
Specific heat of Li_2O_2	$C_{p,\mathrm{Li_2O_2}}$	1.81 J g^{-1} K^{-1}
Thermal conductivity of electrolyte	k_{EL}	0.2 W m^{-1} K^{-1}
Thermal conductivity of electrode	k_{ED}	1.5 W m^{-1} K^{-1}
Thermal conductivity of Li_2O_2	$k_{\mathrm{Li_2O_2}}$	14.5 W m^{-1} K^{-1}
Molecular weight of lithium	M_{Li}	6.94 g mol^{-1}
Molecular weight of lithium peroxide	$M_{\mathrm{Li_2O_2}}$	45.88 g mol^{-1}
Molecular weight of TEGDME	M_{EL}	222.28 g mol^{-1}
Thickness of the electrode MPL	δ_{MPL}	110 μm
Thickness of the electrode GDL	δ_{GDL}	300 μm
Thickness of the separator	δ_{El}	675 μm
Thickness of Li_2O_2 film	$\delta_{\mathrm{Li_2O_2}}$	12 nm
Electric conductivity of Li_2O_2 film	$\sigma_{\mathrm{Li_2O_2}}$	10^{-13} S m^{-1}
Vapor pressure of TEGDME	P_{EL}	1.33 Pa
Width of the battery	δ_y	1 mm
Width of the rib	δ_{Rib}	0~1 mm

Boundary C represents the interface of the cathode electrode and the separator, and flux of oxygen in *x*-direction is zero through this boundary. It was assumed that lithium ion kept at the reference concentration at this boundary.

Boundary D is the interface of the rib and cathode electrode with zero flux of both oxygen and lithium ions. Boundary E is the interface of the cathode electrode and oxygen, where the flux of lithium ion was zero and the oxygen concentration was set to the reference concentration.

In the first part of the study, the electrode was assumed to be saturated with electrolyte during the whole discharge process. In the second part, the electrolyte level changed due to the evaporation of the electrolyte and its effect on battery performance at different open ratios was studied. To model the change of the electrolyte level, it was assumed that the electrode-oxygen interface moved towards the left (the separator) by the rate of V_{EL}, calculated from Eq. 21. This interface was the combination of the boundaries D and E. The oxygen concentration was set as the reference concentration, while the flux of lithium ion was set as zero at this moving boundary. Because of the high thermal conductivity of the lithium anode and battery frame, the temperature at boundaries C and D were assumed to be the room temperature. The heat flux

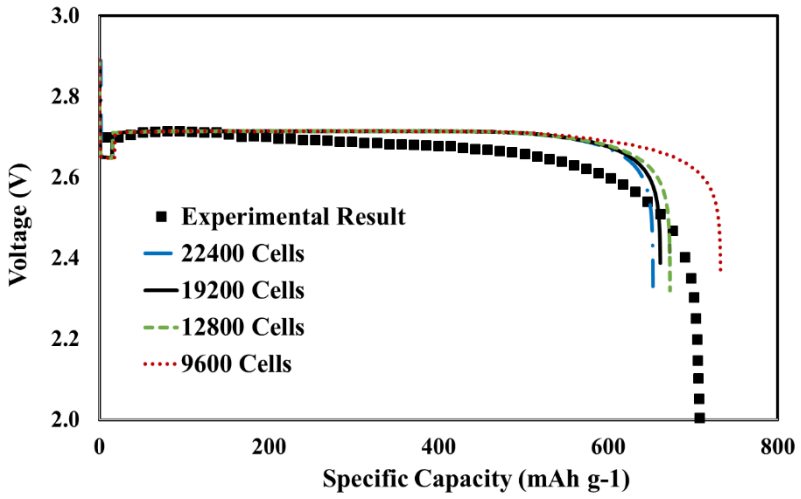

Fig. 3-3. Convergence study of the present model, including both grid independency and time independency of the numerical solution.

through the boundary E (the electrode-oxygen interface) was determined by the natural convection coefficient and the room temperature. All the parameters used in this study are summarized in Table 3-II with their symbols.

3-4. Solution Method and Model Validation:

The computational domain was meshed with quadrilateral grids and based on finite volume method (FVM). Ansys Fluent (release 15.0) was used to create the geometry, generate the mesh, and solve governing equations with given boundary conditions. All the auxiliary equations were defined with a home developed code using C++ and implemented in Ansys Fluent as the user defined functions (UDF). The governing transport equations were solved as the user defined scalar (UDS) and the output data were processed by Ansys Fluent for contour plots and by Microsoft Excel for other charts. Due to velocity criteria in this model, a pressure based solver was selected to linearize and solve the discretized equations [22]. A transient method was used to solve the governing equations and the over-potential was adjusted to maintain a constant discharge current density at each time step. All the transport parameters, including porosity, diffusivity, source terms, active area of the electrode etc. were updated at each individual cell based on the new rate of ORR, accumulated Li_2O_2 and concentrations of species.

The simulation error can be reduced by increasing the number of grid cells and decreasing the time step size. However, these changes tend to increase the computational time and expense. In order to evaluate the sensitivity of the numerical solution on the number of cells and value of the time step, the simulation had been carried out with different numbers of cells (from 9600 to 22400) and time steps (from 2 to 0.5 seconds). The grid number of 19200 and the time step of 1 second were selected for the scope this work, as the refinement of grid number and time step resulted in less than 1% change of the discharge capacity. The grid independent

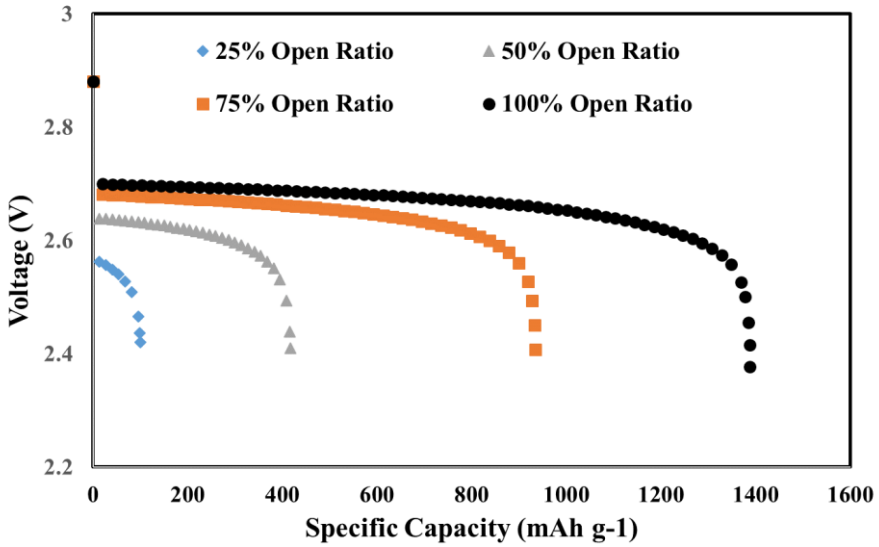

Fig. 3-4. Voltage vs. specific discharge capacity, 0.1 mA/cm^2, constant electrolyte level, various electrode open ratios of 25%, 50%, 75% and 100%

results of a battery with 50% open ratio and discharged at 0.1 mA/cm^2 are presented in Fig. 3-3 to compare with the polarization curve of our experiments at the same condition.

3-4-1. Simulation Results with Constant Electrolyte Level

Different methods can be implemented to keep electrolyte level nearly unchanged: a spring load can be used to eliminate the gap between anode and separator due to anode volume change or a cathode protective layer can be used to reduce the solvent evaporation rate. In this section, it was assumed that electrolyte level remained unchanged and the oxygen electrode was completely saturated with the solvent throughout the discharge process. Simulation results of the specific discharge capacity vs. voltage with different cathode open ratios are plotted in Fig. 3-4. The battery voltage and the specific discharge capacity increased with the increasing open ratio as expected. The maximum discharge capacity increased from 99.7 mAh/g_{carbon} to 1387 mAh/g_{carbon} when the open ratio increased from 25% to 100%. This is due to the limited oxygen diffusivity in the liquid electrolyte. Oxygen is mainly consumed at the cathode/oxygen interface because of the disproportionate oxygen transport rate and oxygen consumption rate. More reaction sites are utilized when the open ratio of the electrode is increased.

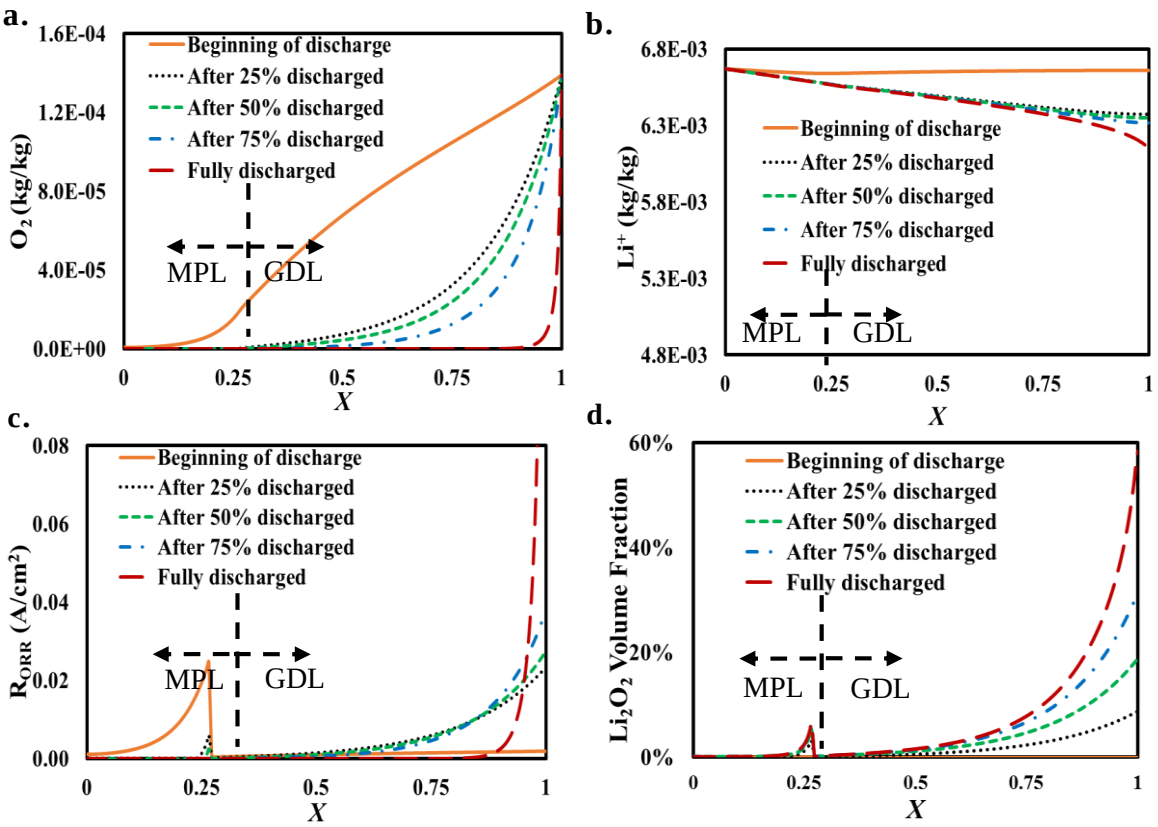

Fig. 3-5. Simulation results without electrolyte level change, 50% open ratio at 0.1 mA/cm^2, Distributions of: a. Oxygen concentration, b. Li^+ concentration, c. Rate of ORR, d. Li_2O_2 volume fraction along electrode length at various discharge steps.

The oxygen concentration along the centerline of the electrode (between separator and oxygen interface) with a 50% cathode open ratio is plotted in Fig. 3-5a. Oxygen had the highest concentration at electrode/air interface due to the limited oxygen diffusivity in the electrolyte. At the beginning of the discharge process, the rate of the ORR is maximum at the GDL/MPL interface, due to the high specific surface area and sufficient oxygen. As shown in Fig. 3-5b, the maximum rate of ORR moves toward electrode/oxygen interface due to the reduced oxygen concentration deep in the electrode. The rate of ORR and the volume fraction of Li_2O_2 are presented in Fig. 3-5c and Fig. 3-5d, respectively. As shown in Fig. 3-5d, Li_2O_2 mainly deposits at the oxygen inlet, which reduces the oxygen diffusivity and further reduces O_2 concentration in the electrode close to the separator and under the ribs. This figure shows that most of the electrode surface area further from the air inlet remains unused. As a result, electrodes with the same thickness but higher open ratios would have a better utilization due to a sufficient oxygen

supply. A two-dimensional contour plot of the volume fraction of Li_2O_2 in an electrode with 50% open ratio at the end of discharge cycle is presented in Fig. 3-8a. As shown in the figure, with constant electrolyte level, the volume fraction of the Li_2O_2 was the highest at electrode/oxygen interface. This volume fraction rapidly diminished at spots further from oxygen opening. The volume fraction of Li_2O_2 was low under the ribs and next to separator. This shows that the higher specific capacity of the battery with higher open ratio was the result of better utilization of the electrode pores by improving oxygen transport.

3-4-2. Simulation Results with Electrolyte Level Change.

To consider the loss of electrolyte caused by evaporation and volume change of the solid, this model simulated the case in which the electrolyte/oxygen interface moved towards the separator during discharge. The speed of the electrolyte/oxygen interface was determined by the flow rate of oxygen and the open ratio of the oxygen electrode. Simulation results in Fig. 3-6 show that by increasing the open ratio from 25% to 100%, the specific discharge capacity decrease from 842 mAh/g_{carbon} to 517 mAh/g_{carbon} at 0.1 mA/cm^2 and 0.1 sccm air flow rate. The simulation results were consistent with our experimental observation that the change of the electrolyte level could significantly affect the discharge performance of the battery.

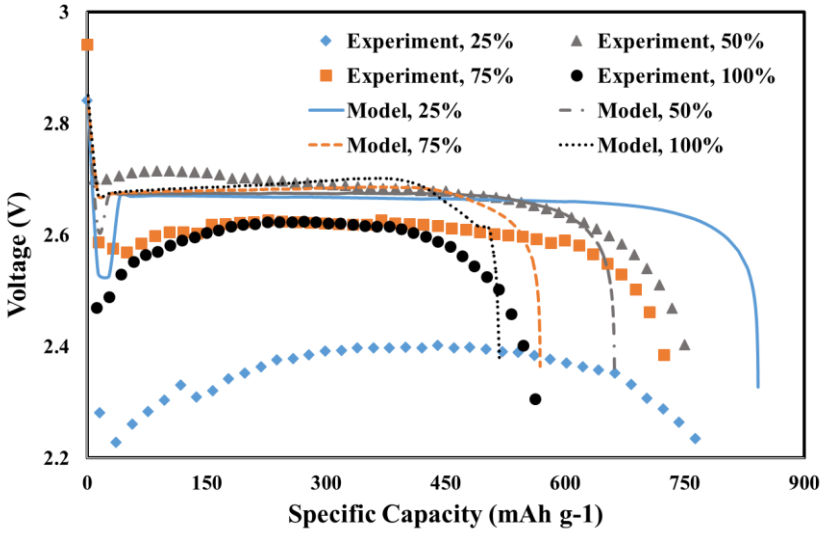

Fig. 3-6. Voltage vs. specific discharge capacity, various electrode open ratios of 25%, 50%, 75% and 100% and Oxygen flow rate of 0.1 sccm, comparison between model and our previous experimental results.

The mass fraction of O_2 along the centerline of the cathode electrode with 50% open ratio, discharged at 0.1 mA/cm^2 and oxygen flow rate of 0.1 sccm is shown in Fig. 3-7a, as the electrolyte level changes, oxygen can migrate further through cathode toward the separator because of the much higher diffusivity of the oxygen in the gas phase in comparison to the oxygen diffusivity in a liquid electrolyte. At the beginning of the discharge, the rate of ORR is high at the MPL/GDL interface, as well as at the electrode/oxygen interface. This can be explained by the higher specific surface area of the cathode at the MPL and sufficient O_2 and Li^+ throughout the cathode. As the battery discharged, Li^+ concentration is reduced near the oxygen side because of the reduced electrolyte level, which is demonstrated in Fig. 3-7b. The rates of ORR, Fig. 3-7c, was reduced at electrode/oxygen interface. The maximum rate of ORR always took place at the MPL/GDL interface because of the increased oxygen concentration

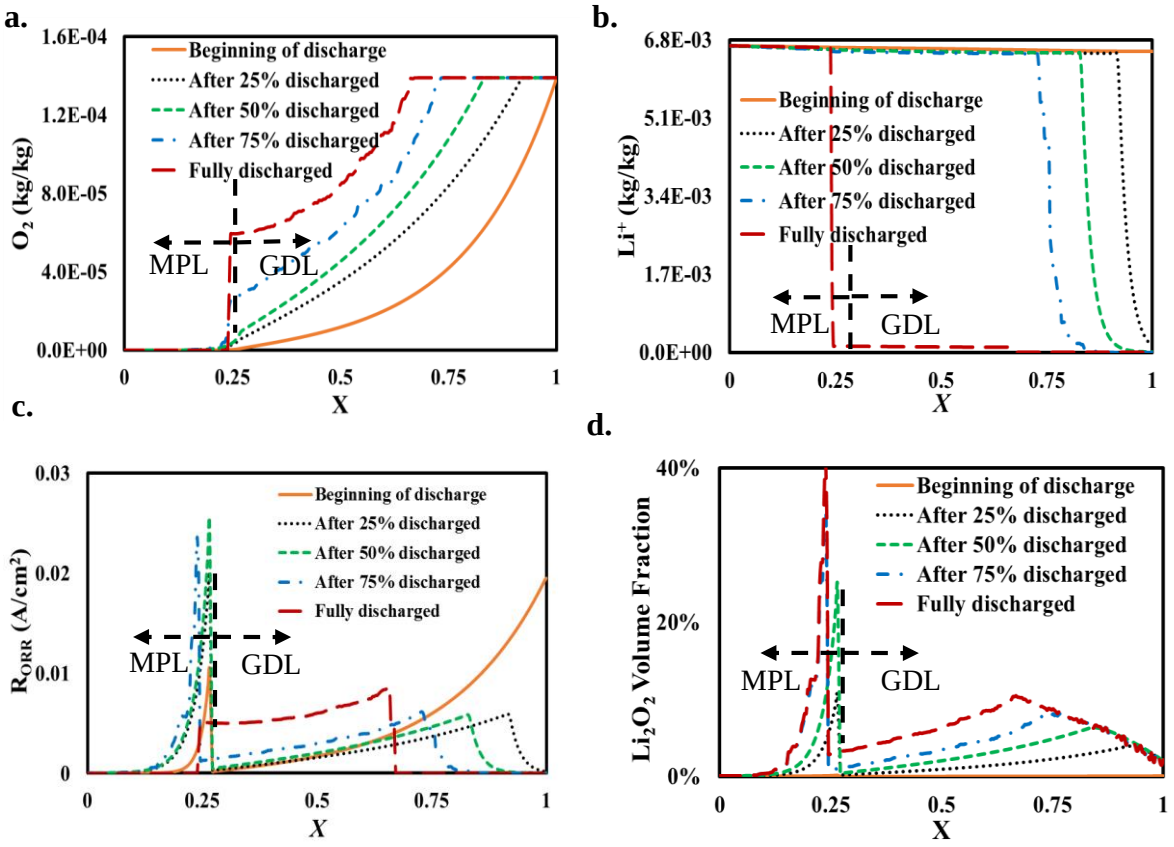

Fig. 3-7. Simulation results with electrolyte level change with 0.1 sccm oxygen flow rate, 50% open ratio at 0.1 mA/cm^2, Distributions of: a. Oxygen concentration, b. Li^+ concentration, c. Rate of ORR, d. Li_2O_2 along electrode length at various discharge steps.

inside the cathode. Due to the Li_2O_2 deposition and pore blockage within the MPL close to the MPL/GDL interface, the concentration of the O_2 was decreased at the MPL/GDL interface and the rate of ORR slowly increased at the moving cathode/oxygen interface. The volume fraction of the Li_2O_2 deposition is shown in Fig. 3-7d. A two-dimensional contour plot of Li_2O_2 volume fraction under the same situation at the end of battery discharge is represented in Fig. 3-8b. As this figure shows, the Li_2O_2 deposition is distinctive from the previous case in which the electrode is fully saturated by the electrolyte (Fig. 3-7). In Fig. 3-8b, discharge products are mainly precipitated at the MPL/GDL interface more interior pores are utilized, and discharge products are more evenly distributed in *y*-direction.

3-5. Conclusions

In this study, a two-dimensional, transient model was developed to study the effect of the open ratio of the oxygen electrode. The electrolyte level change, due to the loss of electrolyte by evaporation and the volume change of the solid, was considered in the model. Simulation results match with the trend observed in specific discharge capacity of our previous experimental results, when the open ratio varied between 25% and 100%. After investigating the effect of evaporation rate at different open ratios, following conclusions can be made:

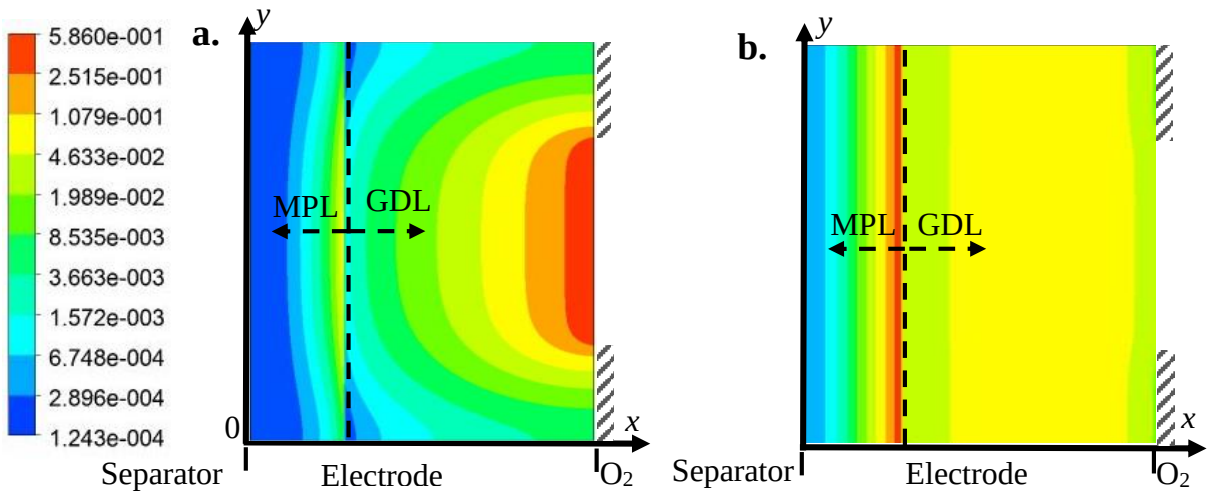

Fig. 3-8. Volume fraction of Li_2O_2 in the cathode with 50% open ratio after fully discharged at 0.1 mA/cm^2: a. without electrolyte level change. b. with electrolyte level change, with oxygen flow rate of 0.1 sccm.

1. When the electrode was fully saturated with the electrolyte, the oxygen concentration was the limiting factor on the battery discharge capacity. The vast majority of the discharge products (Li_2O_2) deposited at the ration
2. electrode/oxygen interface and further reduced the oxygen flux to the interior pores of the electrode. As a result, only a small portion of the cathode is utilized.
3. The discharge capacity of Li-O_2 battery can be significantly increased by increasing the cathode open ratio when the electrolyte fully saturated the electrode. The discharge capacity increased significantly from 99.7 to 1387 mAh g^{-1}, when the open ratio increased from 25% to 100%.
4. The electrode/oxygen interface moves towards the separator due to the evaporation of electrolyte and the volume change of the solid. The oxygen transfer within the electrode partially filled with the electrolyte was remarkably improved since oxygen diffusivity in the gas phase is several orders of magnitude higher than that in the electrolyte. This would result in faster rates of ORR and Li_2O_2 formation at the interior pores. In commercially available electrodes with the MPL, the maximum ORR and Li_2O_2 generation rates were at the MPL/GDL interface because of its high specific surface area in comparison to the GDL substrate.
5. When the evaporation of the electrolyte was considered, the discharge capacity of Li-O_2 battery was decreased by increasing the cathode open ratio. The discharge capacity decreased from 842 to 517 mAh g^{-1} when the open ratio increased from 25% to 100% when the battery discharged at 0.1 mA/cm^2 with 0.1 sccm oxygen flow rate. The decrease of the capacity was caused by the fact that a significant fraction of the electrode was dry during the discharge if the evaporation of the electrolyte was too fast. The evaporation rate of the electrolyte could be engineered by selecting solvents with various vapor pressure, adjusting

the mass transfer resistance of the oxygen selection layer at the cathode, and optimizing the oxygen flow rate.

Reference

[1] K. Abraham, Z. Jiang, A polymer electrolyte-based rechargeable lithium/oxygen battery, Journal of The Electrochemical Society. 143 (1996) 1–5.

[2] J. Read, K. Mutolo, M. Ervin, W. Behl, J. Wolfenstine, A. Driedger, et al., Oxygen transport properties of organic electrolytes and performance of lithium/oxygen battery, Journal of The Electrochemical Society. 150 (2003) A1351–A1356.

[3] C.O. Laoire, S. Mukerjee, K. Abraham, E.J. Plichta, M.A. Hendrickson, Influence of nonaqueous solvents on the electrochemistry of oxygen in the rechargeable lithium- air battery, The Journal of Physical Chemistry C. 114 (2010) 9178–9186.

[4] F. Mohazabrad, F. Wang, X. Li, Experimental Studies of Salt Concentration in Electrolyte on the Performance of Li-O_2 Batteries at Various Current Densities. J. of Power Sources, Under Review., (2016).

[5] X. Li, A. Faghri, Optimization of the cathode structure of lithium-air batteries based on a two-dimensional, transient, non-isothermal model, Journal of The Electrochemical Society. 159 (2012) A1747–A1754.

[6] L. Ye, X. Wang, W. Lv, J. Fei, G. Zhu, Y. Liang, et al., Analytical insight into the oxygen diffusion in wetted porous cathodes of Li-air batteries, Energy. 93 (2015) 416–420.

[7] K. Yoo, S. Banerjee, P. Dutta, Modeling of volume change phenomena in a Li-air battery, Journal of Power Sources. 258 (2014) 340–350.

[8] J. Huang, A. Faghri, Analysis of electrolyte level change in a lithium air battery, Journal of Power Sources. 307 (2016) 45–55.

[9] O. Crowther, M. Salomon, Oxygen selective membranes for li-air (o2) batteries., Membranes (Basel). 2 (2012) 216–27. doi:10.3390/membranes2020216.

[10] J. Jiang, H. Deng, X. Li, S. Tong, P. He, H. Zhou, Research on Effective Oxygen Window Influencing the Capacity of Li-O2 Batteries, ACS Applied Materials \& Interfaces. 8 (2016) 10375–10382.

[11] R.R. Mitchell, B.M. Gallant, C.V. Thompson, Y. Shao-Horn, All-carbon-nanofiber electrodes for high-energy rechargeable Li-O 2 batteries, Energy \& Environmental Science. 4 (2011) 2952–2958.

[12] A. Faghri, Y. Zhang, Transport phenomena in multiphase systems, Academic Press, 2006.

[13] M. Andisheh-Tadbir, M. El Hannach, E. Kjeang, M. Bahrami, An analytical relationship for calculating the effective diffusivity of micro-porous layers, International Journal of Hydrogen Energy. 40 (2015) 10242–10250.

[14] X. Li, A Modeling Study of the Pore Size Evolution in Lithium-Oxygen Battery Electrodes, Journal of The Electrochemical Society. 162 (2015) A1636–A1645.

[15] V. Viswanathan, K.S. Thygesen, J. Hummelshøj, J.K. Nørskov, G. Girishkumar, B. McCloskey, et al., Electrical conductivity in Li2O2 and its role in determining capacity limitations in non-aqueous Li-O2 batteries, The Journal of Chemical Physics. 135 (2011) 214704.

[16] A.B. Anderson, J. Roques, S. Mukerjee, V.S. Murthi, N.M. Markovic, V. Stamenkovic, Activation energies for oxygen reduction on platinum alloys: Theory and experiment, The Journal of Physical Chemistry B. 109 (2005) 1198–1203.

[17] X. Li, J. Huang, A. Faghri, A critical review of macroscopic modeling studies on Li O 2 and Li-air batteries using organic electrolyte: Challenges and opportunities, Journal of Power Sources. 332 (2016) 420–446.

[18] C. Tran, X.-Q. Yang, D. Qu, Investigation of the gas-diffusion-electrode used as lithium/air cathode in non-aqueous electrolyte and the importance of carbon material porosity, Journal of Power Sources. 195 (2010) 2057–2063.

[19] Y.-C. Lu, D.G. Kwabi, K.P. Yao, J.R. Harding, J. Zhou, L. Zuin, et al., The discharge rate capability of rechargeable Li-O 2 batteries, Energy \& Environmental Science. 4 (2011) 2999–3007.

[20] W. Xu, J. Xiao, J. Zhang, D. Wang, J.-G. Zhang, Optimization of nonaqueous electrolytes for primary lithium/air batteries operated in ambient environment, Journal of the Electrochemical Society. 156 (2009) A773–A779.

[21] L.M. Trejo, M. Costas, D. Patterson, Effect of molecular size on the W-shaped excess heat capacities: oxaalkane-alkane systems, Journal of the Chemical Society, Faraday Transactions. 87 (1991) 3001–3008.

[22] ANSYS, Ansys Fluent Theory Guide, Release 15.0, (2013).

Chapter 4. Experimental Studies of Salt Concentration in Electrolyte on the Performance of Li-O_2 Batteries at Various Current Densities

This study experimentally investigated the effects of the salt concentration in an electrolyte on the electrochemical performance of a Li-O_2 battery at various current densities. Electrolyte solutions, made from bis(trifluoromethane)sulfonimide lithium salt (LiTFSI) in tetraethylene glycol dimethyl ether (TEGDME), with different concentrations between 0.005 M and 1 M were tested in the experiment. The viscosity and ionic conductivity of these electrolytes were measured. The first discharge-charge cycle tests were performed on Li-O_2 batteries at current densities from 0.1 to 0.5 mA/cm^2. Both the discharge and charge capacities, as well as the columbic efficiency, decreased with increasing current density. Results also showed that specific discharge and charge capacities of batteries at a low salt concentration ($\leq$ 0.25 M) were also low due to insufficient oxygen and lithium ions along with the slow diffusion of lithium ions in electrolytes. It was found that the balance between ionic conductivity and oxygen concentration determines that the optimized salt concentration for the highest discharge/charge capacities, at the specified current density. At a lower current density ($\leq$ 0.2 mA/cm^2), the highest capacity was obtained with the 0.75 M electrolyte, while at a higher current density (0.3-0.5 mA/cm^2), the highest capacity was obtained with 1 M electrolyte.

4-1. Introduction

Li-O_2 batteries have received significant interest as one of the more promising technologies for energy storage in the past few years due to its high theoretical energy density (1700 Wh/kg) as compared with those of Li-ion batteries [1-3]. Abraham and Jiang [4] first reported a Li-O_2 battery using organic electrolytes since Li-O_2 aqueous electrolyte batteries suffered from metal corrosion by water. Generally, a rechargeable organic electrolyte Li-O_2 battery is composed of a lithium metal anode, a separator saturated with the organic electrolyte, and a porous cathode electrode (typically made from carbon or catalysts). During discharge, the lithium metal is

oxidized to lithium ions at the anode, shown as Eq. (1). Meanwhile, oxygen from the surroundings dissolve in the liquid electrolyte, react with lithium ion, and generate solid Li_2O_2 in the cathode electrode, as shown in Eq. (2). During the charging process, the reversed cathodic reaction decomposes lithium peroxide and releases oxygen and lithium ion. The reversed anodic reaction deposits lithium metal at the anode electrode. The overall reaction is shown in Eq. (3) and the theoretical voltage, E^0, of the reaction is 3.1 V [5].

$$\text{Anode: } 2Li \rightarrow 2Li^+ + 2e^- \quad (1)$$

$$\text{Cathode: } 2Li^+ + 2e^- + O_2 \rightarrow 2Li_2O_2 \quad (2)$$

$$\text{Overall: } 2Li + O_2 \rightarrow 2Li_2O_2 \quad (3)$$

The same electrochemical reactions take place in Li-air batteries [6, 7], in which O_2 is breathed from the ambient air. However, since CO_2 and H_2O in the air would react with the active components in these batteries and deteriorate the performance, most laboratory experiments are conducted under pure O_2 environment. This experimental study was also carried out using pure oxygen and the term Li-O_2 battery is used throughout this paper [8-11]. Researches that focus on electrolyte solvents, lithium salts, catalysts and operating conditions have been carried out to increase the energy density, improve the efficiency, and extend the cycle life of non-aqueous Li-O_2 batteries [5].

Many studies on electrolyte solvents and lithium salts indicated that more stable non-aqueous electrolyte solvents and lithium salts are needed to improve the performance of reversible Li-O_2 batteries [12-16]. In this area, Xu et al. [12] investigated effects of different organic electrolytes, including ethylene carbonate (EC), propylene carbonate (PC), triglyme (TEGDME), butyl diglyme (BDG), dimethyl sulfoxide (DMSO), triethyl phosphate (TEPa) and sebaconitrile, on the discharge performance and discharge products of Li-O_2 batteries. The results showed that Li_2O_2, which is required for the reversible reaction of Li-O_2 batteries, was the main product only in glymes (BDG and TEGDME) among all the investigated solvents. A

large portion of products such as LiF and Li_2CO_3 were generated by side reactions in other solvents. As a result, the coulombic efficiency and cycle life of these batteries were significantly decreased. McCloskey et al. [13] also studied the role of electrolyte solvents such as EC, PC and dimethyl ether (DME). Chemical and electrochemical stability of electrolyte with the presence of reaction products of Li_2O_2 and its intermediates are critical to producing truly rechargeable Li-O_2 batteries. Nasybulin et al. [14] studied effects of lithium salts, including lithium tetrafluoroborate ($LiBF_4$), lithium bis(trifluoromethanesulfonyl)-sulfonimide (LiTFSI), lithium trifluoromethanesulfonate (LiTf), lithium perchlorate ($LiClO_4$), etc., on the performance of Li-O_2 batteries and stability of salt anions. Their results indicated that batteries using LiTFSI salt achieved the highest discharge capacity and showed the best cycling performance. Meini et al. [15] charged carbon electrodes with pre-filled Li_2O_2 in electrolytes made from several solvents and found that ether-based electrolytes were more likely to decompose with the presence of oxygen and high potential. Thus, Li-O_2 batteries with ether-based electrolytes cannot perform as well as those with glymes electrolytes. Geaney and O'Dwyer [16] showed that when galvanostatic tests were conducted in the ambient environment, compared with tests in pure O_2 environment, the discharge capacity of batteries with TEGDME electrolyte solvent increased while the discharge capacity of batteries with DMSO decreased. As result of this literature search, this study used the LiTFSI salt dissolved in TEGDME as the electrolyte due to their high stabilities.

The concentration of the lithium salt in the electrolyte can also significantly influence the performance of non-aqueous Li-O_2 batteries. For example, Liu et al. [17] applied a LiTFSI lithium salt in DME (with the salt concentration of 1 M, 2 M, and 3 M) as the electrolyte in Li-O_2 batteries. Their results showed that high-concentration electrolytes could enhance the stability and reversibility of Li-O_2 batteries by mitigating the decomposition of electrolyte and improve the discharge capacity by reducing the internal resistance. However, a combined

experimental and computational study by Markus et al. [18] indicated that high-concentration electrolytes (> 1 M) resulted in cathode passivation when examining the performance of Li-O_2 batteries with four different LiTFSI lithium salt concentrations of 0.1 M, 1 M, 2 M, and 2.6 M, respectively in DME. Scanning Electron Microscopy (SEM) and Electronic Data System (EDS) analyses indicated that decomposition products in high-concentration electrolytes (> 1 M) coated the cathode surface and led to the sudden death of batteries. The TFSI anion decomposition was more likely to be induced by neutral state, such as the environment in which H^+ and TFSI anion exist and H^+ was formed during decomposition of DME. The authors suggested that non-aqueous Li-O_2 batteries with low-concentration electrolytes and more stable lithium salts obtained higher capacity and better cycle stability. Han et al. [19] conducted research on mixed electrolytes solvent. When the lithium salt concentration increased (from 0.2 M to 1 M), the ionic conductivity decreased, which was different from conductivity changes in conventional electrolytes, and viscosity increased. Adding proper amounts of BMP-TFSI can improve the ionic conductivity and cycle stability by reducing the evaporation of organic electrolyte. Other research by Xu et al. [20] optimized a non-aqueous electrolyte for ambient operations of Li-air batteries. The electrolyte viscosity would increase significantly as the salt concentration increased from 0.5 M to 1.4 M while the ionic conductivity only changed slightly and the peak ionic conductivity was measured at 0.9 M. The highest discharge capacity was obtained when the LiTFSI lithium salt concentration was 0.8 M and electrolyte solvent evaporation loss did not have a significant effect on discharge capacity in a wide range of salt concentrations. Existing studies reached different conclusions of the effect of salt concentration due to the variation of operating conditions, including the current density.

Many studies demonstrated that current density strongly affects the performance of Li-O_2 batteries and higher current densities decreased the cell capacity of batteries [21-30]. Read [21] researched on organic Li-O_2 batteries and experimentally characterized the relationship

between electrolyte and air cathode products and discharge capacity, rate capability, and the rechargeability. When these batteries discharged at various current densities from 0.05 mA/cm^2 to 1.0 mA/cm^2, the discharge capacity decreased almost linearly with the current density. Han et al. [22] utilized 1 M of LiTFSI in diethylene glycol diethyl ether (DEGDEE) as the electrolyte of organic Li-air batteries. The experimental results indicated the discharge voltage plateau decreased by 0.2 V and discharge capacity decreased from 6,219 to 1,251 mAh/g when the current density increases from 0.1 mA/cm^2 to 0.4 mA/cm^2. The charge capacity also decreased with the increasing current density. The experiment conducted by Kumar et al. [23] showed that the discharge and charge capacities were increased by 70% when the current density was decreased from 0.15 mA/cm^2 to 0.1 mA/cm^2. Mirzaeian et al. [24] focused their studies on clarifying effects of operating conditions such as discharge rate, discharge depth and charge taper voltage on the performance of organic Li-O_2 batteries with 1 M $LiPF_6$ in PC. Galvanostatic experiments were conducted under the conditions of various discharge rate from 10 to 150 mA/g. The discharge capacity decreased from 2738 mAh/g to 364 mAh/g as discharge current rate increased from 10 mA/g to 150 mA/g. Concerning the kinetics mechanism, higher discharge current density increased the polarization of the cathode. The cut off voltage and discharge current density also affected the cycling performance of lithium oxygen batteries. Higher discharge current rate (> 70 mA/g) and lower discharge cut off voltage (i.e., 2.05V) resulted in higher initial discharge capacity but the discharge capacity faded more significantly after 15 cycles. Moreover, the study by Grande et al. [25] showed that high charge over-potential led to low coulombic efficiency but the charge over-potential was not affected by the discharge cut off voltage directly. A study conducted by Chen et al. [26] concluded that the discharge capacity of Li-air batteries was mainly limited by the combination of oxygen diffusion and electronic resistance. Batteries discharged at 1 mA/cm^2 at the beginning and 0.2 mA/cm^2 at the end achieved a higher discharge capacity compared with the reversed discharge

process that discharged batteries at 0.2 mA/cm^2 at the beginning and 1.0 mA/cm^2 at the end. Zhang et al. [27] investigated the polarization curve of oxygen electrode in organic Li-O_2 batteries at various current densities ranging from 0.02 to 0.5 mA/cm^2. Discharge capacity was found to decrease with the increase of current density because there was not enough oxygen to enable the discharge reaction at a high current density. Kalubarme et al. [28] and Jadhav et al. [29] studied the discharge capacity of a Li-O_2 battery using 1 M LiTFSI in TEGDME as the electrolyte and perovskite oxide as the catalyst. Discharging performance at current densities from 0.1 to 2 mA/cm^2 showed that discharge capacity decreased with increasing current density, with a sharp decrease from 0.5 to 1 mA/cm^2. The sharp decrease of capacity might be due to the fact that solid reaction products with a lower reactivity covered the surface of the electrode and thus increased the internal resistance and limited the kinetics of the reaction. In addition, it was found that the reaction product distributed uniformly within the electrode at lower current densities and enhanced oxygen diffusion to the electrode as compared with that at higher current densities.

These previous studies indicated that the effects of salt concentration in the electrolyte and the battery performance are strongly related to its operating conditions. Therefore, the optimized lithium salt concentration to obtain the highest capacity is likely determined by the current density. In this chapter, we investigated the discharge and charge capacities of Li-O_2 batteries adopting LiTFSI lithium salt and TEGDME electrolyte solvent. The optimal lithium salt concentration in the electrolyte at various operating current density was obtained after systematically examining the discharge and charge capacities of batteries at various electrolyte concentrations. It should be noted that the decomposition of LiTFSI was not considered in this study since the applied TEGDME is a relative stable solvent and the LiTFSI salt concentration was no more than 1 M.

4-2. Experimental Methodology

Electrolyte preparation. LiTFSI (99.95%) and TEGDME (99%) were both purchased from Sigma Aldrich and used as received. All the electrolytes and salts were stored in a Mikrouna glovebox filled with purified argon (99.9995% purity from Matheson). The water and oxygen concentrations were both kept at less than 1 ppm in the glovebox. Electrolytes were prepared by dissolving LiTFSI in TEGDME with various concentrations in the glovebox. The molar concentration of prepared electrolytes varied from 1 M to 0.005 M.

Battery assembly. The oxygen electrode was made from carbon cloth coated with a microporous layer on one side and purchased from the Fuel Cell Store. The thickness of electrode was 410 µm and the diameter of the electrode was 1.59 cm. A Whatman GF/B glass fiber filter with the diameter of 2.1 cm was used as the separator. The lithium chip with the diameter of 1.56 cm was purchased from MTI Corporation. The frame design of the battery is shown in Fig. 4-1. The current collectors on both the anode and cathode sides were custom-designed and made from highly corrosion-resistant Grade 2 titanium. The PTFE gasket and O-ring were purchased from McMaster-Carr. All batteries were assembled in the glove box by

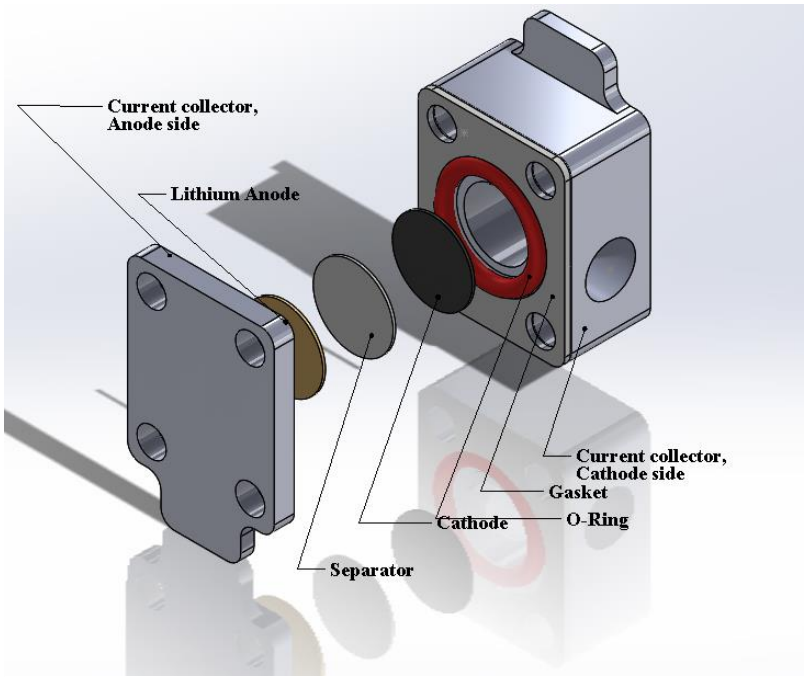

Fig. 4-1. The structure and components of the customized Li-O_2 battery.

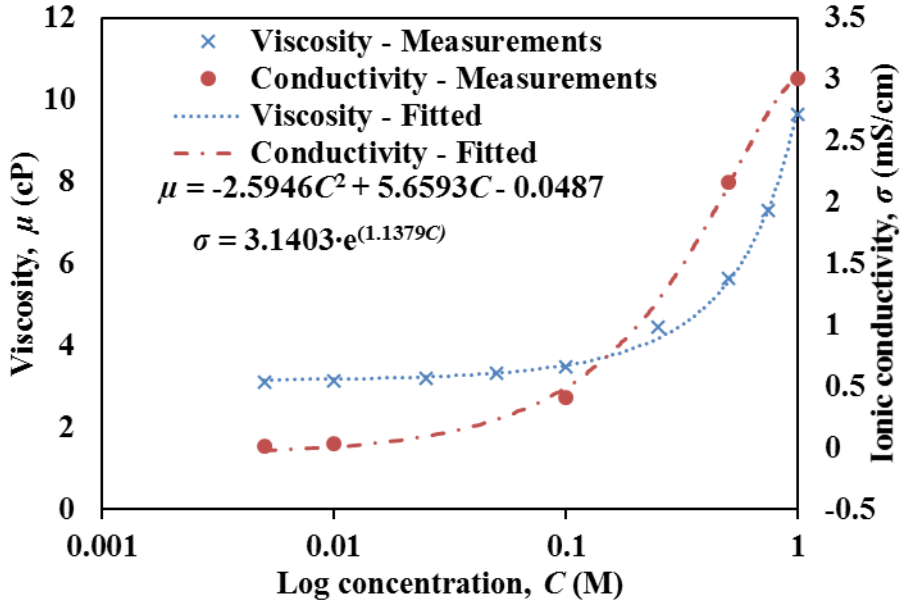

Fig. 4-2. Changes of viscosity and ionic conductivity with LiTFSI salt concentration in TEGDME electrolyte.

adding 65 μL of electrolyte in the separator and in the cathode electrode, respectively. The lithium chip, separator, and the cathode electrode were sandwiched between two customized current collectors (Fig. 4-1).

Measurements. The viscosity measurements of electrolytes were performed with Brookfield DV-II Pro Viscometer at 25 °C. Each group of measurement started with measuring the viscosity of calibration liquid and was repeated three times. All the discharge-charge tests were conducted using a 4-channel Arbin MSTAT4 battery tester at the room temperature (20°C). All batteries had 1 hour of rest before starting the discharge and charge cycles. The cut-off potentials were 2 V and 4.5 V for discharging and charging, respectively.

4-3. Results and Discussion

This study measured the ionic conductivity of electrolytes, σ, with various concentrations, C, (Fig. 4-2). The ionic conductivity decreased (almost linearly) from 3.01 mS/cm to 0.03 mS/cm when the salt concentration decreased from 1 M to 0.01 M. Based on the ionic conductivity of 0.25 M electrolyte (1.28 S/cm) and current density of 0.5 mA/cm^2, the calculated over-potential was negligible (less than 0.02 V). The study conducted by Read [32]

also indicated that the ionic conductivity only had trivial effects on battery performance. Previous work [33] has shown that the O_2 solubility will not change significantly when the salt concentration in organic electrolytes varies from 0 to 1 M. Thus, the O_2 solubility with respect to different salt concentration electrolytes was not measured in this study.

Table 4-I. Viscosity of electrolyte (LiTFSI in TEGDME) measured at 25 °C.

Concentration (M)	Viscosity (cP)	Oxygen diffusivity ($\times 10^6$) (cm^2/s)
1	9.66+/-0.07	1.87
0.75	7.30+/-0.07	2.47
0.5	5.63+/-0.13	3.20
0.25	4.44+/-0.09	4.06
0.1	3.49+/-0.07	5.17
0.05	3.33+/-0.04	5.41
0.025	3.20+/-0.07	5.63
0.01	3.12+/-0.05	5.77

Measurements of viscosity in Fig. 4-2 show that the electrolyte viscosity increased from 3.12 cP to 9.66 cP as the salt concentration increased from 0.01 M to 1 M. The oxygen diffusivity in the electrolyte decreased with the increase of viscosity and the correlation can be described by the Stokes-Einstein equation:

$$D = \frac{kT}{6\pi\mu a} \tag{4}$$

where k is the Boltzmann constant (1.38×10^{-23} m^2 kg s^{-2} K^{-1}), T is the temperature (298 K) and a is effective hydrodynamic radius of O_2 (1.21 Å [32]). The oxygen diffusivities calculated by

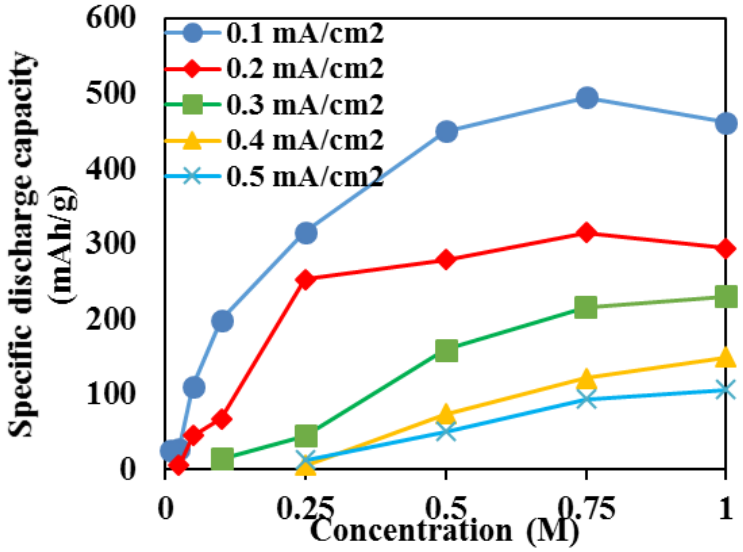

Fig. 4-3. Specific discharge capacities of Li-O_2 batteries at different current densities and electrolyte concentrations.

Eq. (4) and the viscosity measured were also summarized in Table 4-I. Since the oxygen diffusivity is strongly affected by the viscosity, it is crucial to consider the viscosity of the electrolyte to optimize the salt concentration in the electrolyte.

4-3-1. Current Density

Specific discharge capacities of Li-O_2 batteries at different salt concentrations and discharge current densities were measured (Fig. 4-3). The specific discharge and charge capacities in this study were calculated based on the weight of the microporous layer (13.0 mg) of the cathode electrode. Fig. 4-3 indicates that the specific discharge capacity decreased as the discharge current density increased at all electrolyte concentrations. For instance, when the current density increased from 0.1 mA/cm^2 to 0.5 mA/cm^2, the specific discharge capacity decreased from 461.53 mAh/g to 106.07 mAh/g with 1M electrolyte. This trend is consistent with conclusions from existing studies. The concentration over-potential is higher at greater discharge current density because the consumption rate of oxygen and lithium ion by the oxygen reduction reaction is proportional to the current density. As a result, the discharge capacity decreases with the current density. A similar trend of charge capacity with the current density can be observed and will be discussed later.

4-3-2. Electrolyte Concentration

Results in Fig. 4-3 also indicate that the optimized salt concentration to achieve high specific discharge capacity of Li-O_2 batteries is dependent on the discharge current density due to the fact that the electrochemical reaction is influenced by the diffusion rates of oxygen, as well as lithium ions. As shown in the figure, specific discharge capacities decrease sharply when the salt concentration was lower than 0.25 M at all current densities. When the salt concentration decreased from 0.25 M to 0.1 M, the discharge capacity decreases from 252.77 mAh/g to 67.21 mAh/g at 0.1 mA/cm^2 and discharge capacities decrease to almost zero at 0.4 and 0.5 mA/cm^2. This is because a lower salt concentration leads to a reduced Li^+ diffusivity

[34] and a sharp decrease of Li^+ concentration at the reaction sites in the cathode electrode where Li^+ is consumed by the oxygen reduction reaction (ORR). The concentration over-potential of Li^+ increases and the discharge capacity decreases. Therefore, the lithium salt concentration should be higher than 0.25 M to avoid high concentration over-potential and achieve reasonable discharge and charge capacities.

When the salt concentration is above 0.5 M, however, the change of specific discharge capacity with the salt concentration is dependent on the current density. The highest specific discharge capacities were not necessarily achieved with the highest salt concentration. At current densities of 0.1 and 0.2 mA/cm^2, the highest capacities were both obtained at the salt concentration of 0.75 M. The specific capacity decreased by 30 mAh/g when the salt concentration further increased to 1M. At higher discharge current densities (0.3 to 0.5 mA/cm^2), the batteries achieved the highest specific discharge capacities with 1M electrolyte. Furthermore, discharge capacities only had a small increase at high current densities when the salt concentration was above 0.75 M. For example, the specific discharge capacity obtained at 0.3 to 0.5 mA/cm^2 only increased by 20 mAh/g compared with increment of 50 mAh/g when salt concentration changed from 0.5 M to 0.75 M. Electrolytes with higher salt concentrations have a higher viscosity that can hinder O_2 diffusion so that there is not enough O_2 penetrating through the cathodic electrode making their way to the reaction sites. Meanwhile, higher salt concentration provides more Li^+ with higher Li^+ diffusivity. The balance between oxygen diffusivity and availability of Li^+ determines that the highest discharge capacity is dependent on the operating current density and may not be achieved with a higher salt concentration. In

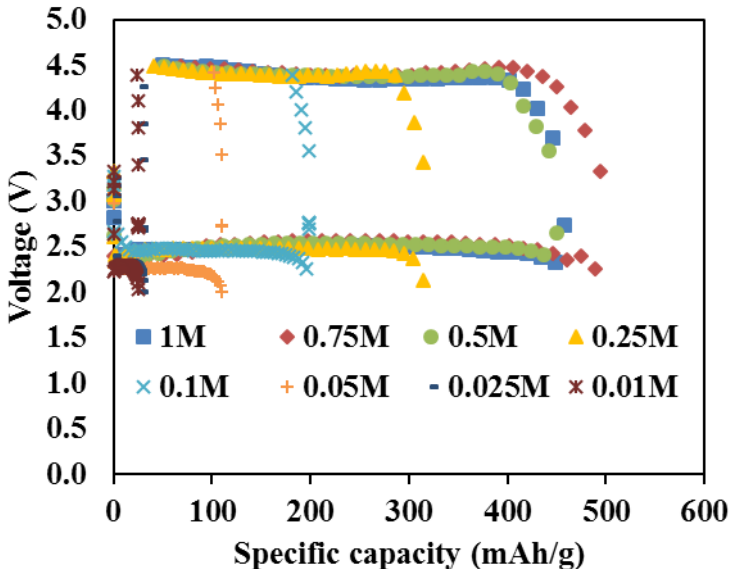

Fig. 4-4. The first discharge-charge cycles of Li-O_2 batteries with different electrolyte concentrations at 0.1 mA/cm^2.

this study, the highest specific discharge capacity was obtained with electrolytes with 0.75 M salt concentration at current densities of 0.1 and 0.2 mA/cm^2.

4-3-3. The First Discharge-Charge Cycle

The first discharge and charge cycles of Li-O_2 batteries at 0.1 mA/cm^2 are shown in Fig.4-4. Both the discharge and charge capacities increased when the salt concentration increased. When the salt concentration increased from 0.5 M to 1.0 M, the charge capacities increased from 273.70 to 407.64 mAh/g. The calculated coulombic efficiencies at 0.1 mA/cm^2, Fig. 4-5, were approximately 90%. However, the charge capacities were less than 20 mAh/g and the

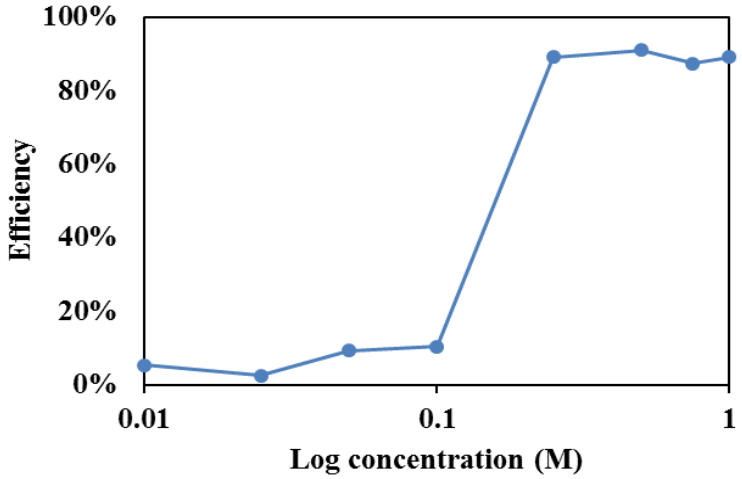

Fig. 4-5. Coulombic efficiencies of Li-O_2 batteries at 0.1 mA/cm^2.

coulombic efficiency were only about 10% with a salt concentration lower than 0.25 M. During charging, Li_2O_2 is decomposed in the cathode electrode through the oxygen evolution reaction and generates Li^+ and e^-. Meanwhile, Li^+ and e^- react at the surface of lithium metal and form Li metal at the anode. The oxygen evolution reaction is more sluggish, compared with the oxygen reduction reaction, due to its high energy barrier. The slow oxygen evolution reaction and insufficient Li^+ for the anode reaction [35] limit the charge performance of the battery. The concentration over-potential of the anode reaction (caused by Li^+) was higher when the salt concentration decreased. As a result, electrolytes with low salt concentrations (less than 0.25 M) result in low charge capacity (and poor rechargeability). To further prove the impact of concentration over-potential at the anode, the discharge and charge over-potentials of a symmetric cell with only lithium electrodes (Li|separator|Li) and various electrolyte solution concentrations (1M, 0.1M, and 0.01 M) were measured at current densities of 0.1, 0.3, and 0.5 mA/cm^2. The over-potential increased (from 0.47, to 0.832 and 2.0 V) when the electrolyte concentration decreased from 1 M to 0.1 M, and 0.001 M at the current rate of 0.1 mA/cm^2. Similarly, the over-potential increased from 0.73V to 2.0V when the electrolyte solution concentration decreased from 1 M to 0.1 M at 0.3 mA/cm^2. Since both electrodes were made

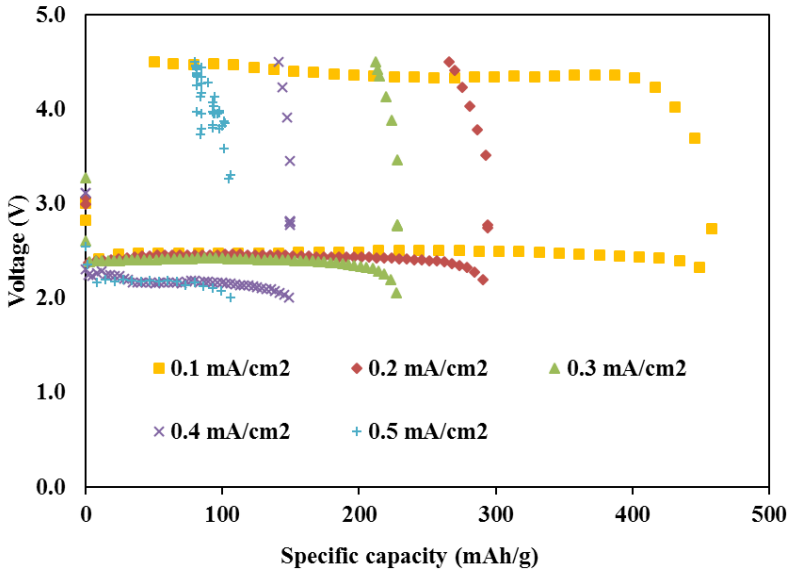

Fig. 4-6. The first discharge-charge cycles of Li-O_2 batteries with 1M electrolyte at various current densities.

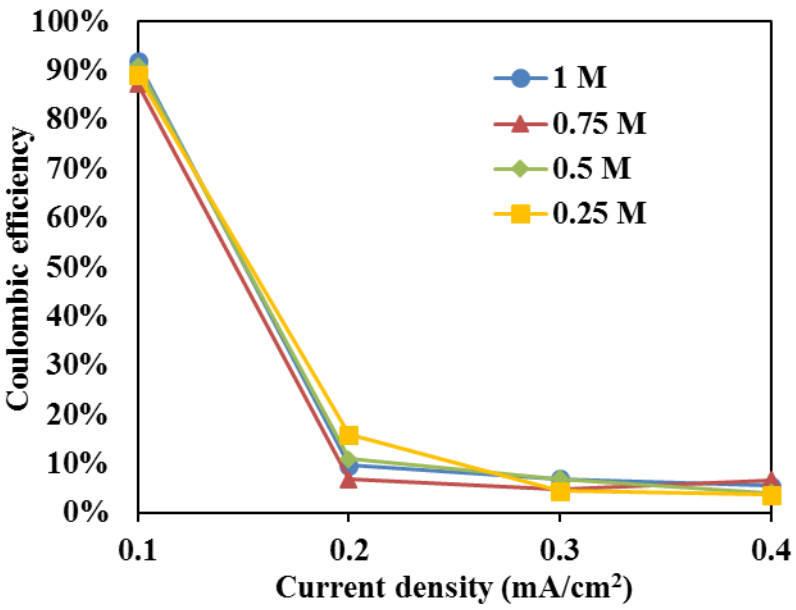

Fig. 4-7. Coulombic efficiencies of Li-O_2 batteries with various electrolyte concentrations.

from lithium metal, the difference resulted from the mass transfer and Ohmic resistances of the lithium metal (the anode electrode in the Li-O_2 battery). Fig. 4-6 shows the discharge-charge profiles of Li-O_2 batteries at various current densities with 1 M electrolyte and Fig. 4-7 compares the coulombic efficiencies of these batteries with electrolytes from 0.25 M to 1 M. When the current rate is higher than 0.2 mA/cm^2, the coulombic efficiency, shown in Fig. 4-7, is less than 20%. At high current rates, the specific discharge capacity is mainly limited by the insufficient concentration rate of O_2. Similarly, the limited concentration rate of Li^+ and the low generation of Li^+ caused by the sluggish kinetics of oxygen evolution reaction leads to low charge capacity. The Li-O_2 battery is expected to be operated at a lower current density to improve both the charge and discharge capacities. The efficiency of discharge-charge cycles decreases with the number of cycles. Since the first discharge-charge cycles showed relative low efficiencies with low lithium salt concentrations, the cyclability of battery after the first cycle was not studied in this work.

4-4. Conclusion

In this study, discharge and charge capacities and the columbic efficiencies of Li-O_2 batteries were studied experimentally with organic electrolytes with different lithium salt concentrations at various current densities. When the salt concentration changed, both the viscosity and lithium ion diffusivity in electrolytes changed that affect the electrochemical performance (discharge and charge capacities) of Li-O_2 batteries. Low specific capacity and weak rechargeability with low salt concentration electrolyte (≤0.25 M) is caused by the insufficient transfer of lithium ion to reaction sites. The specific discharge capacity and rechargeability will be improved significantly when the salt concentration is higher than 0.25 M. On the other hand, the specific discharge capacity slightly decreased when the salt concentration increased from 0.75 M to 1 M at 0.1 and 0.2 mA/cm^2, which indicates that the effect of viscosity increase may counter or even outweigh that of diffusivity increase of lithium ion. The electrochemical performance will also deteriorate when these batteries discharge-charge at higher current densities (> 0.2 mA/cm^2) mainly because of the concentration over-potential caused by limited oxygen and lithium ion transfer. The cumulative results highlight the need to optimize the salt concentration based on the applied current density and clarify the mechanism of capacity and rechargeability change.

Reference

[1] Girishkumar, G.; McCloskey, B.; Luntz, A.; Swanson, S.; Wilcke, W., Lithium− air battery: promise and challenges. *The Journal of Physical Chemistry Letters* **2010,** *1* (14), 2193-2203.

[2] Laoire, C. O.; Mukerjee, S.; Abraham, K.; Plichta, E. J.; Hendrickson, M. A., Elucidating the mechanism of oxygen reduction for lithium-air battery applications. *The Journal of Physical Chemistry C* **2009,** *113* (46), 20127-20134.

[3] Xu, W.; Xiao, J.; Wang, D.; Zhang, J.; Zhang, J.-G., Effects of nonaqueous electrolytes on the performance of lithium/air batteries. *Journal of The Electrochemical Society* **2010,** *157* (2), A219-A224.

[4] Abraham, K.; Jiang, Z., A polymer electrolyte-based rechargeable lithium/oxygen battery. *Journal of The Electrochemical Society* **1996,** *143* (1), 1-5.

[5] Lu, J.; Lau, K. C.; Sun, Y.-K.; Curtiss, L. A.; Amine, K., Review—Understanding and Mitigating Some of the Key Factors that Limit Non-Aqueous Lithium-Air Battery Performance. *Journal of The Electrochemical Society* **2015,** *162* (14), A2439-A2446.

[6] Zhang, J.-G.; Wang, D.; Xu, W.; Xiao, J.; Williford, R. E., Ambient operation of Li/Air batteries. *Journal of Power Sources* **2010,** *195* (13), 4332-4337.

[7] Wang, Y.; Zhou, H., To draw an air electrode of a Li–air battery by pencil. *Energy & Environmental Science* **2011,** *4* (5), 1704-1707.

[8] Lei, Y.; Lu, J.; Luo, X.; Wu, T.; Du, P.; Zhang, X.; Ren, Y.; Wen, J.; Miller, D. J.; Miller, J. T., Synthesis of porous carbon supported palladium nanoparticle catalysts by atomic layer deposition: application for rechargeable lithium–O_2 battery. *Nano letters* **2013,** *13* (9), 4182-4189.

[9] Qin, Y.; Lu, J.; Du, P.; Chen, Z.; Ren, Y.; Wu, T.; Miller, J. T.; Wen, J.; Miller, D. J.; Zhang, Z., In situ fabrication of porous-carbon-supported α-MnO_2 nanorods at room temperature: application for rechargeable Li–O_2 batteries. *Energy & Environmental Science* **2013,** *6* (2), 519-531.

[10] Adams, B. D.; Radtke, C.; Black, R.; Trudeau, M. L.; Zaghib, K.; Nazar, L. F., Current density dependence of peroxide formation in the Li–O_2 battery and its effect on charge. *Energy & Environmental Science* **2013,** *6* (6), 1772-1778.

[11] Lu, J.; Qin, Y.; Du, P.; Luo, X.; Wu, T.; Ren, Y.; Wen, J.; Miller, D. J.; Miller, J. T.; Amine, K., Synthesis and characterization of uniformly dispersed Fe_3O_4/Fe nanocomposite on porous carbon: application for rechargeable Li–O_2 batteries. *Rsc Advances* **2013,** *3* (22), 8276-8285.

[12] Xu, W.; Hu, J.; Engelhard, M. H.; Towne, S. A.; Hardy, J. S.; Xiao, J.; Feng, J.; Hu, M. Y.; Zhang, J.; Ding, F., The stability of organic solvents and carbon electrode in nonaqueous Li-O_2 batteries. *Journal of Power Sources* **2012,** *215*, 240-247.

[13] McCloskey, B.; Bethune, D.; Shelby, R.; Girishkumar, G.; Luntz, A., Solvents' critical role in nonaqueous lithium–oxygen battery electrochemistry. *The Journal of Physical Chemistry Letters* **2011,** *2* (10), 1161-1166.

[14] Nasybulin, E.; Xu, W.; Engelhard, M. H.; Nie, Z.; Burton, S. D.; Cosimbescu, L.; Gross, M. E.; Zhang, J.-G., Effects of electrolyte salts on the performance of Li–O_2 batteries. *The Journal of Physical Chemistry C* **2013,** *117* (6), 2635-2645.

[15] Meini, S.; Solchenbach, S.; Piana, M.; Gasteiger, H. A., The role of electrolyte solvent stability and electrolyte impurities in the electrooxidation of Li_2O_2 in Li-O_2 batteries. *Journal of The Electrochemical Society* **2014,** *161* (9), A1306-A1314.

[16] Geaney, H.; O'Dwyer, C., Examining the Role of Electrolyte and Binders in Determining Discharge Product Morphology and Cycling Performance of Carbon Cathodes in Li-O_2 Batteries. *Journal of The Electrochemical Society* **2016,** *163* (2), A43-A49.

[17] Liu, B.; Xu, W.; Yan, P.; Sun, X.; Bowden, M. E.; Read, J.; Qian, J.; Mei, D.; Wang, C. M.; Zhang, J. G., Enhanced Cycling Stability of Rechargeable Li–O_2 Batteries Using High-Concentration Electrolytes. *Advanced Functional Materials* **2016,** *26* (4), 605-613.

[18] Markus, I. M.; Jones, G.; García, J. M., Investigation of Electrolyte Concentration Effects on the Performance of Lithium–Oxygen Batteries. *The Journal of Physical Chemistry C* **2016,** *120* (11), 5949-5957.

[19] Han, S.-M.; Kim, J.-H.; Kim, D.-W., Cycling Performances of Lithium-Air Cells Assembled with Mixed Electrolytes of Ionic Liquid and Diethylene Glycol Diethyl Ether. *Journal of The Electrochemical Society* **2015,** *162* (2), A3103-A3109.

[20] Xu, W.; Xiao, J.; Zhang, J.; Wang, D.; Zhang, J.-G., Optimization of nonaqueous electrolytes for primary lithium/air batteries operated in ambient environment. *Journal of the Electrochemical Society* **2009,** *156* (10), A773-A779.

[21] Read, J., Characterization of the lithium/oxygen organic electrolyte battery. *Journal of The Electrochemical Society* **2002,** *149* (9), A1190-A1195.

[22] Han, S.-M.; Kim, J.-H.; Kim, D.-W., Evaluation of the Electrochemical Performance of a Lithium-Air Cell Utilizing Diethylene Glycol Diethyl Ether-Based Electrolyte. *Journal of The Electrochemical Society* **2014,** *161* (6), A856-A862.

[23] Kumar, B.; Kumar, J.; Leese, R.; Fellner, J. P.; Rodrigues, S. J.; Abraham, K., A solid-state, rechargeable, long cycle life lithium–air battery. *Journal of The Electrochemical Society* **2010,** *157* (1), A50-A54.

[24] Mirzaeian, M.; Hall, P. J.; Sillars, F. B.; Fletcher, I.; Goldin, M. M.; Shitta-bey, G. O.; Jirandehi, H. F., The Effect of Operation Conditions on the Performance of

Lithium/Oxygen Batteries. *Journal of the Electrochemical Society* **2013,** *160* (1), A25-A30.

[25] Grande, L.; Paillard, E.; Hassoun J.; Park J.; Lee Y.; Sun Y.; Passerini S., Scrosati, B., The lithium/air battery: still an emerging system or a practical reality? Advanced materials 2015, 27(5), A784-A800.

[26] Chen, X.; Bevara, V.; Andrei, P.; Hendrickson, M.; Plichta, E.; Zheng, J., Combined effects of oxygen diffusion and electronic resistance in Li-air batteries with carbon nanofiber cathodes. *Journal of The Electrochemical Society* **2014,** *161* (12), A1877-A1883.

[27] Zhang, D.; Fu, Z.; Wei, Z.; Huang, T.; Yu, A., Polarization of oxygen electrode in rechargeable lithium oxygen batteries. *Journal of the Electrochemical Society* **2010,** *157* (3), A362-A365.

[28] Kalubarme, R. S.; Park, G.-E.; Jung, K.-N.; Shin, K.-H.; Ryu, W.-H.; Park, C.-J., LaNixCo1-xO_3-δ Perovskites as Catalyst Material for Non-Aqueous Lithium-Oxygen Batteries. *Journal of The Electrochemical Society* **2014,** *161* (6), A880-A889.

[29] Jadhav, H. S.; Kalubarme, R. S.; Roh, J.-W.; Jung, K.-N.; Shin, K.-H.; Park, C.-N.; Park, C.-J., Facile and cost effective synthesized mesoporous spinel $NiCo_2O_4$ as catalyst for non-aqueous lithium-oxygen batteries. *Journal of The Electrochemical Society* **2014,** *161* (14), A2188-A2196.

[30] Li, X.; Faghri, A., Optimization of the cathode structure of lithium-air batteries based on a two-dimensional, transient, non-isothermal model. *Journal of The Electrochemical Society* **2012,** *159* (10), A1747-A1754.

[31] Li, X., A modeling study of the pore size evolution in lithium-oxygen battery electrodes. *Journal of The Electrochemical Society* **2015,** *162* (8), A1636-A1645.

[32] Read, J.; Mutolo, K.; Ervin, M.; Behl, W.; Wolfenstine, J.; Driedger, A.; Foster, D., Oxygen transport properties of organic electrolytes and performance of lithium/oxygen battery. *Journal of The Electrochemical Society* **2003,** *150* (10), A1351-A1356.

[33] Baird, W. R.; Foley, R. T., Solubility of oxygen in selected organic solvents. *Journal of Chemical and Engineering Data* **1972,** *17* (3), 355-357.

[34] Lee, S.-I.; Jung, U.-H.; Kim, Y.-S.; Kim, M.-H.; Ahn, D.-J.; Chun, H.-S., A study of electrochemical kinetics of lithium ion in organic electrolytes. *Korean Journal of Chemical Engineering* **2002,** *19* (4), 638-644.

[35] Lu, Y.-C.; Gallant, B. M.; Kwabi, D. G.; Harding, J. R.; Mitchell, R. R.; Whittingham, M. S.; Shao-Horn, Y., Lithium–oxygen batteries: bridging mechanistic understanding and battery performance. *Energy & Environmental Science* **2013,** *6* (3), 750-768.

Chapter 5. Conclusions and Future Work

5-1. Summary

In this study, experimental and modeling methods were used to investigate mass transport properties of a Li-O_2 battery. The influence of oxygen cathode open ratio and lithium salt concentration on the discharge-charge specific capacity of a battery at various current densities were experimentally examined. The effects of these factors separately and in combination with other factors are demonstrated. Multiple approaches are proposed to optimize the battery performance based on its applications and working conditions.

Limited oxygen transfer within the cathode is one of the main reasons for the slow discharge reaction rate and for the reduced specific capacity of the battery. For the same reason, discharge products are mainly deposited at the cathode/oxygen interface. It was expected that increasing the oxygen opening size would increase the battery specific capacity by improving the mass transfer of oxygen. Our experiments in the second chapter of this work showed that other factors, such as electrolyte evaporation and/or ohmic contact resistance can balance the effects of the increased open ratio. Both electrolyte evaporation and contact resistance are proportional to the cathode open ratio. It was also shown that current density is another factor that determines the optimum cathode open ratio. There are many other factors that can affect the results of this experiment: e.g., cathode wettability and oxygen flow rate. With our experiment setup and battery components used, the best discharge capacity was obtained at 25% open ratio when the batteries discharged at 0.1 mA/cm^2 and at 3% open ratio when discharged at 3 mA/cm^2. EIS methods were used to demonstrate how contact resistance increased with increased open ratio. Different initial amounts of electrolyte were used at the same open ratio, to demonstrate the importance of electrolyte level in the electrode (electrolyte level is a function of the initial amount of electrolyte and evaporation rate).

A novel model that considers the evaporation of electrolyte at various electrode open ratios has been developed in the third chapter of this work. This model can predict the trend of the discharge capacities at various open ratios observed by our experiments. Electrolyte level changed is caused by evaporation and the volume change of solid lithium to Li_2O_2. Modeling results indicated that when the electrode was fully saturated with the electrolyte, the oxygen concentration was the limiting factor on the battery discharge capacity. The vast majority of the discharge products (Li_2O_2) deposited at the electrode/oxygen interface and further reduced the oxygen flux to the interior pores of the electrode. As a result, only a small portion of the cathode pore volume was utilized. The discharge capacity of Li-O_2 battery can be significantly increased by increasing the cathode open ratio when the electrolyte fully saturates the electrode. If the electrolyte level change was considered in the model, the electrode/oxygen interface moved towards the separator due to the evaporation of electrolyte. The oxygen transport within the electrode partially filled with the electrolyte was remarkably improved since the oxygen diffusivity in the gas phase is several orders of magnitude higher than that in the electrolyte. This would result in faster rates of ORR and Li_2O_2 formation at the interior pores. In commercially available electrodes with the MPL, the maximum ORR, and Li_2O_2 generation rates was at the MPL/GDL interface because of its high specific surface area in comparison to the GDL substrate. When the evaporation of the electrolyte was considered, the discharge capacity of Li-O_2 battery was decreased by increasing the cathode open ratio.

The influence of the salt concentration is studied in the fourth chapter of this study. Both the viscosity and lithium ion diffusivity in electrolytes are related to the salt concentration. Viscosity was reduced by decreasing the lithium salt concentration. The diffusivity of dissolved species is inversely proportional to the viscosity and so the mass transfer was expected to improve slightly. On the other hand, the ionic conductivity of the electrolyte was greatly decreased by decreasing the salt concentration, especially for the salt concentration below 0.25

M. Electrochemical performance (discharge and charge capacities) of Li-O_2 batteries was a function of various factors including the current density. Low specific capacity and weak rechargeability with low salt concentration electrolyte (≤0.25 M) was caused by the insufficient transfer of lithium ion to reaction sites. Results indicated that at low current densities (≤ 0.2 mA/cm^2), the effect of increased viscosity may counter or even outweigh that of the diffusivity increase of lithium ion and slightly lower salt concentration than 1 M (the ideal salt concentration for the current densities ≥ 0.2 mA/cm^2) was needed.

5-2. Recommendation for Future Work

1. More experiments are required to quantify the electrolyte evaporation rate and validate its combined effects with the open ratio on the battery discharge capacity. Different methods can be used for this study: 1) cathode protective layer can be used at cathode/oxygen interface to reduce the evaporation rate, 2) Different amount of electrolyte can be added while the oxygen flow remained unchanged, 3) different oxygen flow can be used (when the initial amount of electrolyte remained unchanged), 4) a more hydrophilic cathode electrode can be used, 5) electrolyte can be slowly added to the electrode to keep the electrode saturated during discharge-charge cycle. A comparison between current study (Chapter 2) and the values and trends of discharge capacities obtained from these methods at various open ratios can better validate the effects of open ratio and evaporation rate on the battery performance.
2. A novel model with evaporation term in conjunction with various open ratios has been developed in Chapter 2 of this study. In this model, it was assumed that electrolyte uniformly evaporates at the electrode/oxygen interface. Electrolyte level change in a porous media is very complex. A continuous model is unable to simulate this matter. The cathode is a heterogeneous media with mixed wettability. This means some pores might be more hydrophobic or hydrophilic than the others. Actual pore distance from the oxygen entrance

opening is another important factor in electrolyte loss within different pores. The actual distance is a function of the closeness of the pore to the oxygen entrance and the tortuosity of the electrode in that region. Temperature and capillary fingering are among other factors that make the evaporation process more complicated. All these properties change by time and by the rate of ORR and deposited discharge products within the pores. A micro-level model should be developed to better predict the mass transfer of species and availability of electrolyte, O_2, Li^+ and ideal pore size based on the initial detailed pore structure of the electrode.